STEM CELLS TRANSLATIONAL MEDICINE

EMBRYONIC STEM CELLS/INDUCED PLURIPOTENT STEM (iPS) CELLS

Wnt Signaling Orchestration with a Small Molecule DYRK Inhibitor Provides Long-Term Xeno-Free Human Pluripotent Cell Expansion

KOUICHI HASEGAWA,[a,b,c] SHIN-YA YASUDA,[a] JIA-LING TEO,[a] CU NGUYEN,[a] MICHAEL MCMILLAN,[a] CHIH-LIN HSIEH,[d] HIROFUMI SUEMORI,[e] NORIO NAKATSUJI,[c,e] MASASHI YAMAMOTO,[f] TOMOYUKI MIYABAYASHI,[g] CAROLYN LUTZKO,[h] MARTIN F. PERA,[a,b] MICHAEL KAHN[a,i,j,k]

Key Words. DYRK • Wnt • Human embryonic stem cells • Human induced pluripotent stem cells

ABSTRACT

An optimal culture system for human pluripotent stem cells should be fully defined and free of animal components. To date, most xeno-free culture systems require human feeder cells and/or highly complicated culture media that contain activators of the fibroblast growth factor (FGF) and transforming growth factor-β (TGFβ) signaling pathways, and none provide for replacement of FGF/TGFβ ligands with chemical compounds. The Wnt/β-catenin signaling pathway plays an important role in mouse embryonic stem cells in leukemia inhibitory factor-independent culture; however, the role of Wnt/β-catenin signaling in human pluripotent stem cell is still poorly understood and controversial because of the dual role of Wnts in proliferation and differentiation. Building on our previous investigations of small molecules modulating Wnt/β-catenin signaling in mouse embryonic stem cells, we identified a compound, ID-8, that could support Wnt-induced human embryonic stem cell proliferation and survival without differentiation. Dual-specificity tyrosine phosphorylation-regulated kinase (DYRK) is the target of the small molecule ID-8. Its role in human pluripotent cell renewal was confirmed by DYRK knockdown in human embryonic stem cells. Using Wnt and the DYRK inhibitor ID-8, we have developed a novel and simple chemically defined xeno-free culture system that allows for long-term expansion of human pluripotent stem cells without FGF or TGFβ activation. These culture conditions do not include xenobiotic supplements, serum, serum replacement, or albumin. Using this culture system, we have shown that several human pluripotent cell lines maintained pluripotency (>20 passages) and a normal karyotype and still retained the ability to differentiate into derivatives of all three germ layers. This Wnt-dependent culture system should provide a platform for complete replacement of growth factors with chemical compounds. STEM CELLS TRANSLATIONAL MEDICINE *2012;1:18–28*

INTRODUCTION

The goal of regenerative medicine is to repair or replace damaged or diseased tissues or organs. In the past decade, since the first human embryonic stem cells (hESCs) were described [1, 2], there has been remarkable progress toward clinical applications of hESC-derived cellular therapeutics. However, further improvements toward the economical production of large quantities of either hESCs or induced pluripotent stem cells (iPSCs) [3, 4] cultured in fully defined xeno-free conditions remain an important research goal for therapeutic applications. Although several feeder- and xeno-free culture conditions have been reported [5–7], these conditions require complex culture media or many human-derived protein components. In particular, to meet good manufacturing practice (GMP) standards, replacing such components with small molecules would provide significant advantages. The development of well-defined xeno-free culture conditions is contingent upon our understanding of the key signaling pathways involved in hESC self-renewal. The extrinsic factors regulating hESC maintenance and early differentiation events seem to differ from those of mouse embryonic stem cells (mESCs) and to date are incompletely understood [8], but activation of basic fibroblast growth factor (bFGF) and transforming growth factor-β (TGFβ)/Activin/Nodal signaling forms the cornerstone of most systems for hESC propagation [9, 10].

Wnt signaling plays important roles throughout development [11]. Wnt signaling is important in stem cell biology; however, there is no consensus as to whether Wnt signaling is important for differentiation of stem/progenitor cells or proliferation and maintenance of potency (pluripotency or multipotency) [12, 13]. Wnt/β-catenin signaling has been demonstrated to

[a]Eli and Edythe Broad Center for Regenerative Medicine and Stem Cell Research, [b]Department of Cell and Neurobiology, [d]Departments of Urology and Biochemistry and Molecular Biology, Norris Cancer Center, [i]Department of Biochemistry and Molecular Biology, Keck School of Medicine, [j]Department of Molecular Pharmacology and Toxicology, and [k]Center for Molecular Pathways and Drug Discovery, University of Southern California, Los Angeles, California, USA; [c]Institute for Integrated Cell-Material Sciences and [e]Institute for Frontier Medical Sciences, Kyoto University, Sakyo-ku, Kyoto, Japan; [f]Functional Additives Division, Asahi Kasei Chemicals Corporation, Kawasaki, Kanagawa, Japan; [g]Asahi Kasei Medical America Inc., Westbury, New York, USA; [h]Department of Pediatrics, University of Southern California Saban Research Institute, Children's Hospital Los Angeles, Los Angeles, California, USA.

Correspondence: Michael Kahn, Ph.D., Eli and Edythe Broad Center for Regenerative Medicine and Stem Cell Research, University of Southern California, 1425 San Pablo Street, Los Angeles, California 90033, USA. Telephone: 323-442-2063; Fax: 323-442-4040; e-mail: kahnm@usc.edu

Received September 19, 2011; accepted for publication October 26, 2011; first published online in SCTM *EXPRESS* December 7, 2011.

1066-5099/2012/$30.00/0

http://dx.doi.org/10.5966/sctm.2011-0033

maintain pluripotency in mESCs in leukemia inhibitory factor (LIF)-independent culture, but it is dispensable in LIF-dependent culture [14–16]. In hESCs, it has been reported that Wnt/β-catenin signaling maintains cells in the undifferentiated state [12, 17, 18]; however, it has also been reported that Wnt/β-catenin signaling induces differentiation [19, 20]. Thus, the dichotomous behavior of Wnt/β-catenin signaling in controlling both proliferation and differentiation of hESCs has been unclear and has fueled enormous controversy concerning the role of Wnt signaling in maintenance of pluripotency and induction of differentiation.

Using a chemical genomic approach, we have previously identified small molecule chemical compounds that modulate Wnt/β-catenin signaling and developed a model that rationalizes these divergent behaviors as a result of differential transcriptional coactivator binding to β-catenin in various stem cell types, including mESCs [21–23]. Modulation of Wnt/β-catenin signaling provided long-term mESC self-renewal in defined culture conditions without LIF [22, 24]. Therefore, we investigated whether orchestration of Wnt/β-catenin signaling with a small molecule modulator would allow for the long-term growth and maintenance of hESCs under defined xeno-free conditions.

Materials and Methods

Cells and Cell Culture

The hESC lines HES2 [2], HES3 [2], H1 [1], and H9 [1] and the human fetal dermal fibroblast-derived iPSC line [25] were maintained using standard cell culture methodology. For enzymatic bulk expansion, the cells were cultured on mitotically arrested mouse embryonic fibroblast (MEF) feeder cell layers in Dulbecco's modified Eagle's medium/Ham's F-12 medium (DMEM/F-12; Sigma D6421; Sigma-Aldrich, St. Louis, http://www.sigmaaldrich.com) supplemented with 20% knockout serum replacement (KSR; Invitrogen, Carlsbad, CA, http://www.invitrogen.com), L-glutamine, nonessential amino acid, and 4 ng/ml recombinant bFGF2 (fibroblast growth factor 2 [FGF2]; Peprotech, Rocky Hill, NJ, http://www.peprotech.com), as previously described. For feeder-free culture, the MEF feeder layer was removed via separation from embryonic stem cell clumps by sedimentation under gravity during passage, and cells were cultured in MEF-conditioned medium (MEF-CM) on 30-fold diluted Matrigel (BD Biosciences, San Diego, CA, http://www.bdbiosciences.com)-coated culture dishes.

The replating assay was previously described [26]. Briefly, the hESCs in feeder-free culture were dissociated completely with 0.05% trypsin-EDTA (Invitrogen) and seeded at 10^4 cells per well in Matrigel-coated 6-well culture plates and cultured in MEF-CM. Various concentrations of Wnt3a (purchased from Peprotech or prepared in our laboratory on the basis of a previous report [27]; the activity of the purified Wnt3a was confirmed using the super TOPFLASH assay [28]), IQ-1, ID-8, and/or ICG-001 (all synthesized in our laboratory; identity and purity confirmed by proton nuclear magnetic resonance and liquid chromatography/mass spectrometry [LC/MS]) were supplemented into the culture media at the onset of seeding and then continuously until the end of culturing. For all assays, the cell and colony morphology were examined under a microscope, and the replating efficiency was examined by counting the number of colonies after 7 days of culture.

For xeno-free, feeder-free culture, the cells were passaged onto 2 μg/cm^2 human fibronectin (from human foreskin fibroblasts; Sigma-Aldrich F2518), 10–20 μg/cm^2 human laminin (from human fibroblasts; Sigma-Aldrich L4544), and 10 μg/cm^2 human vitronectin (Recombinant Vitoronectin; Invitrogen PHE0011)-coated culture dishes and cultured in DMEM/F-12 (Sigma D6421) supplemented with L-glutamine, nonessential amino acids, insulin-transferrin-selenite (ITS) (Sigma-Aldrich I1884; dosage twice as high as manufacturer's instructions), 1 μg/ml L-ascorbic acid, 20–25 ng/ml Wnt3a, and 500 nM ID-8, with or without 4 ng/ml bFGF. The culture medium was changed daily. Some of the colonies detached from the edge of the dish after 5–7 days of culture. At this time or when colonies became confluent, cells were treated with 0.5 mg/ml GRGDTP peptide (AnaSpec, Fremont, CA, http://www.anaspec.com) or 1 μg/ml echistatin (Sigma-Aldrich) and incubated at 37°C for 15–45 minutes until all colonies started to detach at the edge region. The colonies were detached and partially dissociated into clumps by gentle pipetting, and then the clumps were washed with culture medium, collected by centrifugation, and seeded onto new dishes at a 1:2 or 3 split ratio.

For examination of cell attachment, subconfluent cells were dissociated as clumps, and a part of the solution containing cell clumps was dissociated into single cells with 0.25% trypsin-EDTA for cell counting. The clumps were seeded into 24-well plates with an estimated 5,000-cell clumps per well. After overnight culture, nonattached cells were washed away with phosphate-buffered saline (PBS), attached cells were dissociated with 0.25% trypsin-EDTA, and then the attached cell number was examined. For examination of cell population growth, the cells were seeded into 24-well plates with an estimated 2,000- or 5,000-cell clumps per well, and the cells were dissociated and counted every 24 hours.

Experiments using hESCs and hiPSCs in this study have been approved by University of Southern California Stem Cell Research Oversight Committee (No. 2008-6-1).

Quantitative Polymerase Chain Reaction Analysis

Total RNA was isolated from hESCs cultured in feeder-free conditions with or without Wnt3a and ID-8 using an RNeasy micro kit (Qiagen, Hilden, Germany, http://www1.qiagen.com). Reverse transcription was performed with Omniscript (Qiagen), and quantitative reverse transcription–polymerase chain reaction (PCR) was then performed using each gene-specific primer/probe mix (TaqMan Gene Expression Assays), TaqMan 2 × Master Mix, and the ABI Prism 7900 Sequence Detection system (Applied Biosystems, Foster City, CA, http://www.appliedbiosystems.com) according to the manufacturer's protocol. The PCR data were analyzed by the Δ/Δ C_T method and normalized with Cycrophilin A (PPIA) expression with RQ Manager software (Applied Biosystems).

Identification of ID-8 Target

The cells were washed twice with 5 ml of ice-old PBS, harvested by scraping into 1 ml of PBS containing protease inhibitor cocktail (Calbiochem, San Diego, CA, http://www.emdbiosciences.com) and collected by centrifugation. The cell pellet was frozen and stored in liquid nitrogen. A total of 2 g of cell pellets were collected from 20 dishes each of 15-cm diameter. The pellets were thawed on ice and then suspended in 20 ml of chilled M-Per

buffer (Pierce, Rockford, IL, http://www.piercenet.com) containing 1 mM dithiothreitol (DTT) and the protease inhibitor cocktail. The cell suspension was mixed and lysed on a nutating mixer for 30 minutes at 4°C. The lysate was then centrifuged at 10,000 rpm for 30 minutes at 4°C, and the supernatant was divided into two equal aliquots in 50-ml centrifuge tubes. Dimethyl sulfoxide (DMSO) control was added to one tube, and 100 μM ID-8 was added to the other tube. The tubes were incubated for 1 hour on a nutator at 4°C. Four hundred microliters of a 50% slurry of streptavidin-Sepharose (GE Healthcare Life Sciences, Piscataway, NJ, http://www.gelifesciences.com) was pre-equilibrated in M-Per buffer and then added to 10 ml of 50 μM biotinylated ID-8 and incubated for 1 hour at 4°C. The Sepharose beads were then washed extensively with M-Per to remove unbound biotinylated ID-8. The streptavidin-Sepharose bound with biotinylated ID-8 was mixed with the DMSO- or free ID-8-treated cell lysates described above. The mixture was then incubated on a nutating mixer for 4 hours at 4°C. The Sepharose beads, containing proteins bound to biotinylated ID-8, were washed three times with 1 ml of M-Per buffer and then mixed with 2× Laemmli Sample Buffer and boiled for 5 minutes. The proteins and Sepharose were then separated using Illustra MicroSpin Columns (GE Healthcare Life Sciences). Bound proteins eluted in Laemmli Buffer were subjected to SDS-polyacrylamide gel electrophoresis (PAGE) and silver stained (Invitrogen). The specific bands decreased by free competitor ID-8 were analyzed by LC/MS (LTQ-XL; Thermo Scientific). The elution was also analyzed by Western blotting with specific antibodies against dual-specificity tyrosine phosphorylation-regulated kinase 1a (DYRK1a) (2771; Cell Signaling Technology, Beverly, MA, http://www.cellsignal.com), DYRK2 (ab37912; Abcam, Cambridge, MA, http://www.abcam.com), DYRK3 (sc-66868; Santa Cruz Biotechnology Inc., Santa Cruz, CA, http://www.scbt.com), DYRK4 (ab37911; Abcam), or HIP2K (sc-100383; Santa Cruz Biotechnology).

Knockdown Assay

Several DYRK microRNAs (miRNAs) were designed and lentiviral vector plasmids were constructed using the Block-iT Pol II miR RNAi kit (Invitrogen) according to the manufacturer's protocol. The knockdown efficiencies of the miRNA expression plasmids were evaluated by transient transfection and Western blotting. The most efficient miRNA sequence, antisense, 5′-tcaaggagtcaatttcgtaacg-3′, and sense, 5′-gttacgaatgacctccttg-3′, was used for further lentiviral production.

To produce the miRNA expression lentiviral vectors, the plasmid was cotransfected with packaging plasmids for vesicular stomatitis virus G protein pseudotyped virus into 293T cells with Fugene6 transfection reagent (Roche Applied Science, Indianapolis, IN, http://www.roche-applied-science.com). Viral supernatants were collected and concentrated by ultracentrifugation for 2 hours. Feeder-free H9 cells were infected with the virus in MEF-CM supplemented with 10 μg/ml polybrene. The infected cells were selected and isolated as pools using 0.5–1 μg/ml Blasticidin over 1 week. The infected H9 cell pools were then used for examination of replating efficiency.

Nuclear Purification and Immunoprecipitation

The cells were washed twice with ice-cold PBS, scraped, and harvested following treatment with DMSO control, 500 nM ID-8, or 20 μM ICG-001 for 24 hours. The nuclear fraction was purified using an NE-PER nuclear extraction kit (Pierce, Thermo Scientific). For prevention of protein degradation, 1 mM DTT and a protease inhibitor cocktail (Calbiochem) were supplemented during harvest and processing. A total 5 μg of nuclear protein from each treated sample was then reacted with 1 μg of anti-CREB-binding protein (CBP) antibody (sc-369; Santa Cruz Biotechnology), anti-p300 antibody (sc-584; Santa Cruz Biotechnology), or normal rabbit IgG in 1 ml of immunoprecipitation buffer (25 mM Tris, HCl, pH 7.5, 150 mM NaCl, 5% glycerol, 0.5% Nonidet P40, 1 mM EDTA, 1 mM DTT, and protease inhibitor cocktail) at 4°C overnight. The protein-antibody complex was then reacted with 50 μl of 50% slurry of protein A-agarose beads (Roche Applied Science) on a nutator for 1 hour at 4°C. The bead complex was washed three times with immunoprecipitation buffer, resuspended with 2× Laemmli buffer, and boiled for 5 minutes. The protein and Sepharose were then separated on an Illustra MicroSpin Column (GE Healthcare Life Sciences). Bound proteins eluted in the Laemmli buffer were subjected to SDS-PAGE and transferred onto polyvinylidene difluoride membrane overnight. The coimmunoprecipitated β-catenin was detected by Western blotting with an anti-β-catenin antibody (610153; BD Biosciences). The intensity of the β-catenin Western blotting signal was analyzed using UN-SCAN-IT software (version 5.1, Silk Scientific, Orem, UT, http://www.silkscientific.com) and normalized with the signals in the total nuclear lysate.

Characterization, Karyotype Analysis, and Differentiation Assay

The hESC colonies were fixed with 4% paraformaldehyde (PFA), and alkaline phosphatase (ALP) activity was determined with a Vector Blue Alkaline Phosphatase Substrate Kit (Vector Laboratories, Burlingame, CA, http://www.vectorlabs.com). Immunostaining was carried out with the following primary antibodies: TRA-1–60 and TRA-1–80 (Santa Cruz Biotechnology), anti-stage-specific embryonic antigen (SSEA)-3 and -4 (Developmental Studies Hybridoma Bank, Iowa City, IA, http://www.uiowa.edu/~dshbwww), GCTM-2 (our laboratory), anti-OCT-3 (clone C-10; Santa Cruz Biotechnology), rabbit anti-SOX2 (Millipore, Billerica, MA, http://www.millipore.com), or goat anti-Nanog (R&D Systems Inc., Minneapolis, http://www.rndsystems.com). Then, samples were incubated with Alexa Fluor 488- or 594-conjugateed antibodies (Molecular Probes, Eugene, OR, http://probes.invitrogen.com), and staining was detected by indirect immunofluorescence microscopy.

For fluorescence-activated cell sorting (FACS) analysis, cells were dissociated with TrypLE (Invitrogen), fixed with 2% PFA, and reacted with TRA-1–60 or GCTM-2 antibody followed by Alexa Fluor 488-conjugated anti-mouse IgM antibodies. The stained cells were then analyzed using an LSRII flow cytometer (BD Biosciences).

For karyotyping, hESCs were treated with 100 ng/ml colcemid (KaryoMax; Invitrogen), dispersed, and fixed. Twenty to 50 cells at metaphase in each sample were analyzed for G-banding at the 300–500 band levels following trypsin digestion and Giemsa staining.

For differentiation assays, embryoid bodies (EBs) were formed for 2 weeks in low-attachment culture plates and then plated onto glass culture slides as described previously [26]. After the cells grew out from attached EBs, they were fixed with 4% PFA, incubated with anti-βIII-tubulin (clone TU-20; Chemicon, Temecula, CA, http://www.chemicon.com), anti-glial fibrillary

acidic protein (anti-GFAP; clone 4A11; BD Biosciences), anti-α-smooth muscle actin (αSMA) (clone 1A4; DakoCytomation, Glostrup, Denmark, http://www.dakocytomation.com), anti-Desmin (clone Ab-1; Thermo Scientific), anti-SOX17 (clone 245013; R&D Systems), anti-SOX7 (goat polyclonal; R&D Systems), or anti-α-fetoprotein (AFP) antibody (clone C3; Sigma-Aldrich) as the primary antibodies and then detected using Alexa Fluor 488- or 594-conjugated secondary antibodies (Molecular Probes) and fluorescence microscopy.

For teratoma formation, hESCs were dissociated as clumps, and a 200-μl suspension containing approximately 10^7 cells was subcutaneously injected into SCID mice (Jackson Laboratory, Bar Harbor, ME, http://www.jax.org). After 2–3 months, the resulting teratomas were dissected out and fixed with Bouin's fixative solution. Samples were embedded in paraffin, sectioned at 5-μm thickness, and subsequently stained with hematoxylin and eosin. This study has been approved by the University of Southern California Institutional Animal Care and Use Committee (No. 11273).

RESULTS

Small Molecule ID-8 Supports hESC Maintenance in Combination with Wnt-3a

The effects of the canonical Wnt ligand Wnt3a and several candidate small molecule Wnt signaling modulators were first evaluated briefly in a replating assay [26] (Fig. 1A). In the replating assay, colonies were dissociated into single cells and seeded on Matrigel-coated plates in MEF-CM [29]. We evaluated cell survival by colony number (replating efficiency: colony number/seeded cell number), proliferation by colony size, and the undifferentiated state by morphology and ALP positivity. When HES2 cells [2] were dissociated and seeded in control MEF-CM, the replating efficiency was ~0.6%. Supplementation with Wnt3a enhanced colony formation slightly (~1% at 100 ng/ml). The colonies were larger and consisted of more cells. All the colonies were still ALP positive. However, the cells in the Wnt-treated colonies appeared flatter than with the control non-Wnt conditions (Fig. 1B, 1C). These results suggested that Wnt3a supplementation enhances hESC survival and proliferation but also partially induces differentiation. As anticipated, treatment with the small molecule ICG-001, which directly modulates Wnt/β-catenin signaling by antagonizing the interaction of β-catenin with transcriptional cofactor CBP and enhancing its interaction with transcriptional cofactor p300 [21], strongly induced cell differentiation in the presence or absence of Wnt3a, and almost all colonies were ALP negative. The other modulator, IQ-1, which is sufficient to maintain mESC proliferation and pluripotency for extended periods of time in the absence of serum and LIF in conjunction with Wnt3a by enhancing the CBP/β-catenin association [22], did not significantly affect hESC survival and proliferation by itself even at the highest dose in the nontoxic range (10 μM), although it partially prevented Wnt-induced differentiation. By contrast, the third modulator, ID-8, which was identified in the same screen as IQ-1 [24], increased hESC survival (~1.1% at 0.5 μM). The combination of Wnt3a and ID-8 further increased survival (~1.7%) and completely prevented Wnt-induced differentiation morphologically without disrupting proliferation. Cells treated with this combination expressed pluripotency markers, including ALP, OCT4, NANOG, and SOX2 at essentially the same levels as control hESCs (Fig. 1D, 1F). Wnt-induced differentiation marker gene expression (i.e., GATA6, SOX17, T [Brachyury], GSC [goosecoid] and CDX2) was dramatically reduced by ID-8 at a dose that maintained the undifferentiated state in this assay (Fig. 1G, 1H). To examine the generality of this effect in hESCs, replating assays were performed with the additional hESC lines HES3 [2] and H9 [1] (Fig. 1E). In both, the combination of Wnt and ID-8 enhanced hESC replating efficiency, and colonies expressed ALP and displayed undifferentiated morphology.

ID-8 Targets DYRK in hESCs

We next sought to investigate the molecular targets and mechanism(s) of action of ID-8 in Wnt/β-catenin signaling. To identify the molecular target(s) of ID-8 (Fig. 2A), we used affinity chromatography (Fig. 2B). We identified DYRK2 as a binding partner of ID-8 in cell lysates; its binding to the ID-8 affinity column was competed away by free ID-8. Immunoblotting of the bound proteins identified not only DYRK2 but also DYRK4 (Fig. 2C). These data suggested that these or other members of the DYRK family are critical molecular targets of ID-8 in hESCs. To confirm this, we designed miRNAs to target the DYRK family and evaluated their effects on protein expression after transfection by immunoblotting (Fig. 2D, 2E). The DYRK miRNA-transfected hESCs maintained their undifferentiated state, as did the untransfected or scrambled control miRNA-transfected cells in MEF-CM or on feeders (supplemental information Fig. 1), showing that there was no adverse effect of the miRNA under conditions that support hESC renewal. Next, we performed replating assays with the stably transfected hESCs. Survival and self-renewal were not different between DYRK-knockdown cells and control cells in the absence of Wnt. However, both parameters were enhanced in the DYRK-knockdown cells in the presence of Wnt ligand (Fig. 2F). The effect of DYRK-knockdown was thus very similar to ID-8 treatment in the replating assay. Taken together, these data indicate that members of the DYRK family are direct targets of ID-8 and that ID-8 enhances Wnt-mediated hESC survival and proliferation via inhibition of DYRKs.

Based upon our model and previous investigations in mESCs [22], we anticipated that ID-8 would modulate Wnt/β-catenin signaling through the enhancement of CBP/β-catenin association at the expense of the p300/β-catenin association in hESCs. To test this hypothesis, CBP and p300 were immunoprecipitated from purified nuclear fractions and then coprecipitated β-catenin amount was examined by immunoblotting (Fig. 2G, 2H). As expected, levels of the CBP/β-catenin complex were significantly enhanced in ID-8-treated cells compared with control and in particular to ICG-001-treated cells. A similar result was obtained in DYRK-knockdown cells (Fig. 2I, 2J). We conclude that ID-8, through inhibition of DYRK family members, supports maintenance of the undifferentiated state in the presence of Wnt by modulating Wnt/β-catenin signaling and enhancing the CBP/β-catenin association in hESCs, similar to the mechanism observed in mESCs treated with IQ-1 and Wnt.

ID-8 and Wnt-Based Xeno- and Feeder-Free Culture System for hESCs and Human iPSCs

Because Wnt and IQ-1 could maintain mESCs without serum and LIF [22], we next investigated the development of a xeno-free, feeder-free hESC culture system using ID-8 with Wnt activation. We first examined the maintenance of hESCs in conventional

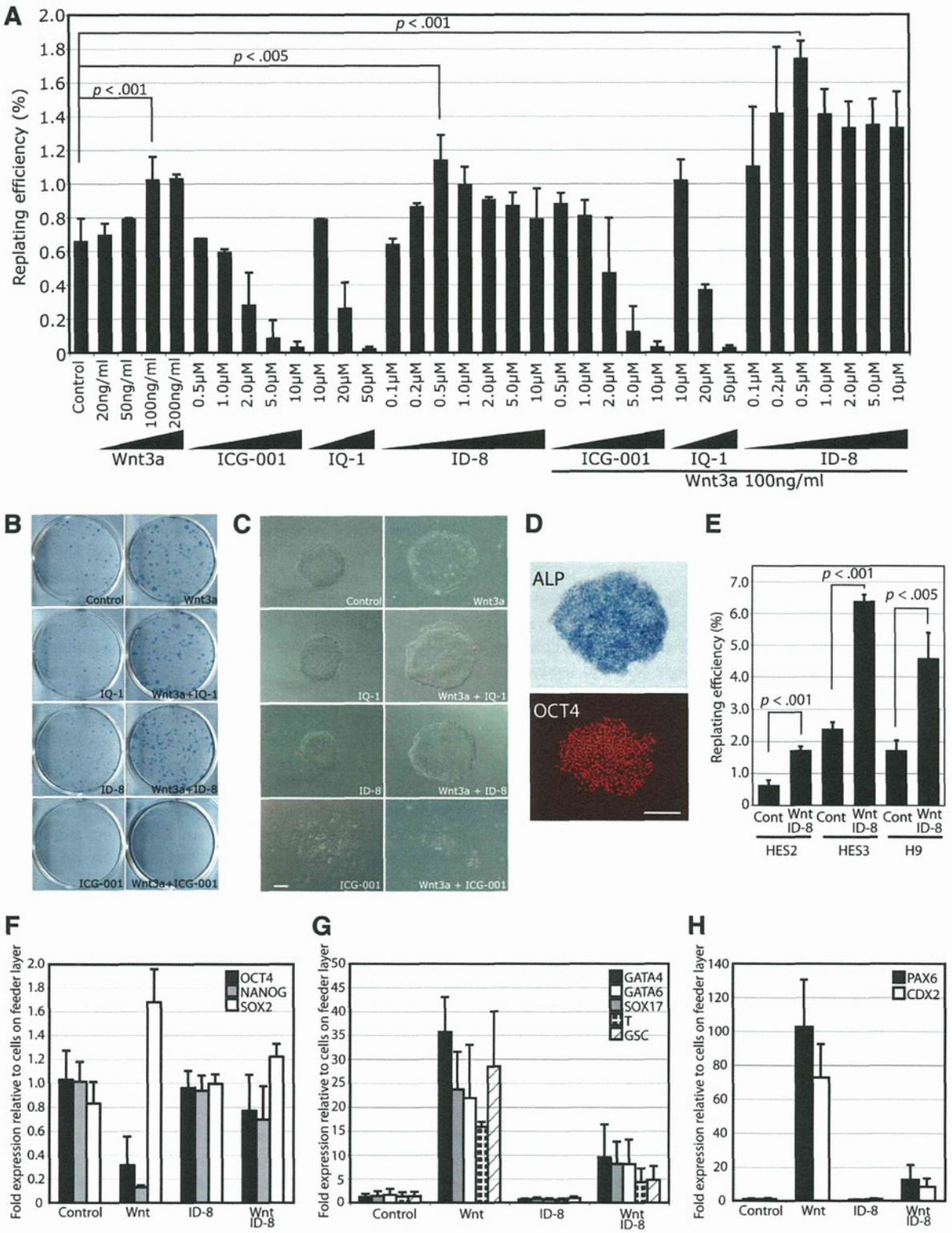

Figure 1. A combination of ID-8 and Wnt ligand enhances human embryonic stem cell (hESC) survival and proliferation. **(A):** Screening of small molecule Wnt signaling modulators in replating assays with HES2 cells in mouse embryonic fibroblast conditioned medium (MEF-CM). Colony numbers per seeded cell numbers indicate replating efficiency. Statistical significance (p value) was calculated by Student's t test. Shown are cultured plates stained with ALP **(B)** and morphologies of typical colonies at day 7 **(C)**. **(D):** ALP staining and OCT4 immunostaining of HES2 cells cultured in MEF-CM with 0.5 μM ID-8 and 100 ng/ml Wnt3a. **(E):** Replating efficiency of HES2, HES3, and H9 cells cultured in MEF-CM with or without ID-8 and Wnt3a. Statistical significance (p value) was calculated by Student's t test. Graphs show quantitative polymerase chain reaction analysis of pluripotent markers **(F)** and differentiation markers **(G, H)** in HES2 cells cultured in MEF-CM with or without ID-8 and Wnt3a. Scale bars = 200 μm; error bars indicate SD. Abbreviation: ALP, alkaline phosphatase.

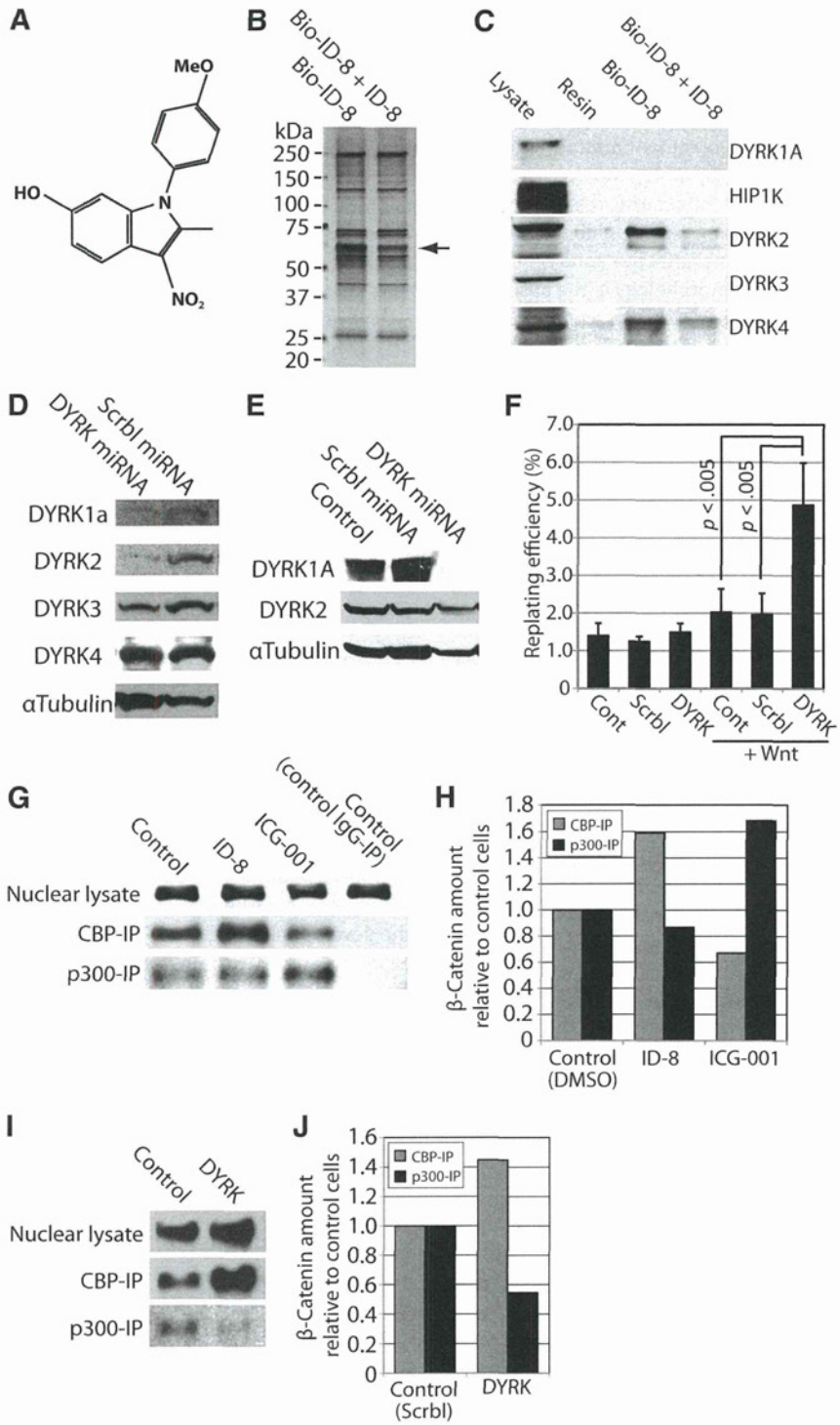

Figure 2. Identification of ID-8 target molecule. **(A):** Molecular structure of ID-8. **(B):** Silver staining of proteins pulled down with biotin-conjugated ID-8 and streptavidin-Sepharose in SDS-polyacrylamide gel electrophoresis. Arrow indicates a specific band (60 kDa) decreased by competition with nonbiotin-conjugated ID-8. **(C):** Western blotting with DYRK family-specific antibodies. Samples were pulled down with resin only, biotin-conjugated ID-8, or biotin-conjugated ID-8 plus nonconjugated ID-8. **(D):** Western blotting with DYRK antibodies after transient transfection of DYRK miRNA or control scrambled miRNA expression plasmid. **(E):** Western blotting of stable transfectants. **(F):** Replating efficiency of H9 human embryonic stem cells (hESCs) stably transfected with miRNA. Error bars indicate SD. Statistical significance (p value) was calculated by Student's t test. **(G):** Western blotting image for coimmunoprecipitation of nuclear β-catenin from ID-8, ICG-001, or nontreated cells with anti-CBP, anti-p300 negative control IgG. **(H):** Band intensity analysis of CBP or p300-associated β-catenin in ID-8- or ICG-001-treated cells relative to nontreated control cells. **(I):** Western blotting image for coimmunoprecipitation of nuclear β-catenin from DYRK miRNA or control scrambled miRNA-transfected cells. **(J):** Band intensity analysis of CBP or p300-associated β-catenin in DYRK miRNA-transfected cells relative to scrambled miRNA-transfected control cells. Abbreviations: Cont, control; DYRK, dual-specificity tyrosine phosphorylation-regulated kinase; IP, immunoprecipitation.

hESC medium, supplemented with Wnt3a and ID-8, and stepwise elimination of bFGF and KSR components, such as albumin, ITS, and ascorbic acid. After extensive investigation, we determined that the minimal medium required to maintain hESC proliferation and pluripotency consisted of DMEM/F-12 with Wnt3a (25 ng/ml), ID-8 (0.5 μM), and ITS (supplemental information Fig. 2A). In the absence of ID-8, Wnt3a, or ITS, no colonies were obtained. L-Ascorbic acid did not affect the maintenance of hESCs in this assay, apart from causing growth inhibition at doses greater than 25 μg/ml. In the minimal effective condition, hESCs maintained their undifferentiated morphology in the absence of bFGF; however, proliferation was significantly enhanced as in MEF-CM by supplementation of 4 ng/ml bFGF (supplemental information Fig. 2A). This concentration of bFGF is much lower than that reported previously for xeno- and feeder-free medium supplemented with bFGF (100 ng/ml) [10].

Initially, we maintained cells on Matrigel, a complex animal-derived extracellular matrix (ECM). However, we investigated various ECM combinations and found that a combination of fibronectin, laminin, and vitronectin (FLV) was best for supporting hESC attachment (supplemental information Fig. 2B) and self-renewal and for maintenance of undifferentiated colony morphology in the medium. Using this ECM combination, the majority of the colonies remained intact up to 7 days in this culture condition, although some colonies tended to detach after 5 days. Therefore, it proved optimal to passage at around 5 days after seeding.

Because of the extremely low level of protein in these cultures (i.e., no albumin or Matrigel), the hESCs are extremely sensitive to damage caused by the dissociation enzymes normally used for passaging, such as collagenase IV, dispase, or trypsin/EDTA. ROCK inhibitor, which has been reported to enhance hESC survival [30], was not very effective under these conditions and also induced differentiation, even with manual mechanical passaging. To develop a passaging process compatible with the very low protein content of our defined medium, we investigated several integrin antagonists. We found that both the synthetic peptide disintegrin GRGDTP and echistatin effectively induced colony detachment and allowed for the passage of hESCs in our medium.

Combining these discoveries, a simple xeno-free and feeder-free culture system was developed incorporating ITS/Wnt3a/ID-8/DMEM/F-12 media, FLV-coated dishes, and disintegrin passaging. Ascorbic acid could be omitted in short-term initial screening; however, we decided to use 1 μg/ml ascorbic acid for additional long-term experiments because it was reported that ascorbate supports hESCs epigenetic status [31]. hESCs transferred into this culture system from normal serum replacement-containing medium were stable and required no culture adaptation. All three hESC lines examined (HES2, HES3, and H9) maintained undifferentiated morphologies for >24 passages (Fig. 3A, passage 17) in this system without bFGF supplementation. The cell proliferation and population doubling rate in these culture conditions without bFGF was slightly lower than that with bFGF (data not shown) or the control MEF-CM (supplemental information Fig. 3A, 3C). All pluripotent stem cells markers examined, including OCT4, SOX2, NANOG, SSEA3, SSEA4, TRA-1–60, TRA-1–81, GCTM-2, and ALP, were expressed in the cells (Fig. 3B). FACS analysis showed that the populations of TRA-1–60- or GCTM-2-positive cells were similar to those maintained under MEF-CM culture conditions (Fig. 3C). Gene expression levels of pluripotent stem cell markers, including OCT4, NANOG, SOX2, and DNMT3B, were not significantly different from those of cells maintained on feeder layers and/or in MEF-CM (Fig. 3D). Normal karyotypes were also maintained in these cells after 22 passages (Fig. 3E). After 17–24 passages, EB-mediated in vitro differentiation and immunostaining for the three germ layer cell markers were performed to evaluate the differentiation capacity of the cultured hESCs (Fig. 4A). These cells readily differentiated into derivatives expressing markers characteristic of all three germ layers, with ectodermal cells expressing βIII-tubulin and GFAP, mesodermal cells expressing αSMA and Desmin, endodermal cells expressing AFP, definitive endodermal cells expressing SOX17 but not expressing SOX7, and extraembryonic endodermal cells expressing SOX7 strongly and SOX17 weakly. In addition, after 22 passages, the cells formed teratomas containing derivatives of all three germ layers when injected subcutaneously into immunodeficient mice (Fig. 4B). In addition to the female hESC cell lines used in the experiments above, a male hESC line H1 [1] and a human dermal fibroblast-derived iPSC line [25] were examined in our culture system. Both cell line cells were maintained in the undifferentiated state for at least 15 passages (Fig. 3A; supplemental information Fig. 3A, 3C). These data suggest that our xeno-free, feeder-free culture system can be used to maintain diploid human pluripotent stem cells long-term.

Discussion

Historically, hESCs or iPSCs have been maintained on MEF feeder layers and in media containing serum or serum replacement [1–4]. These conditions include animal components, and cultures so maintained may be contaminated with pathogens. Therefore, the development of a xeno-free hESC and iPSC culture system is highly desirable for regenerative medicine applications of human pluripotent cells. Several reports have described xeno-free culture systems using human feeders and human serum components [32, 33]. A few additional reports demonstrated xeno-free and feeder-free culture systems for the maintenance of the undifferentiated state of hESCs [5–7]. These culture systems are quite complex and require a large number of human protein components and/or GMP-certified animal components. On the basis of these reports, a few xeno-free and feeder-free culture systems have become commercially available. However, the complexity incurred by the requirement of multiple recombinant proteins, human and/or certified animal components likely will result in cost-prohibitive protocols and more complexities in quality control. A very recent report described a simple xeno-free and feeder-free E8 medium consisting of eight components [10]. Six of the eight components, DMEM/F-12, insulin, transferrin, selenium, ascorbic acid, and $NaHCO_3$ (present in DMEM/F-12), are also included in our medium, but the remaining two, bFGF and TGFβ/Nodal, are not required for our medium, which instead contains Wnt3a and ID-8. Replacement of all recombinant growth factors with chemical compounds, however, would be highly beneficial. However, to date, no previous defined formulation has eliminated the use of bFGF or TGFβ. In addition, several reports have appeared describing the screening of large chemical libraries for small molecules that support hESC renewal [34, 35]; however, to this point, these efforts have not led to a vastly simplified xeno-free culture medium. Because there are

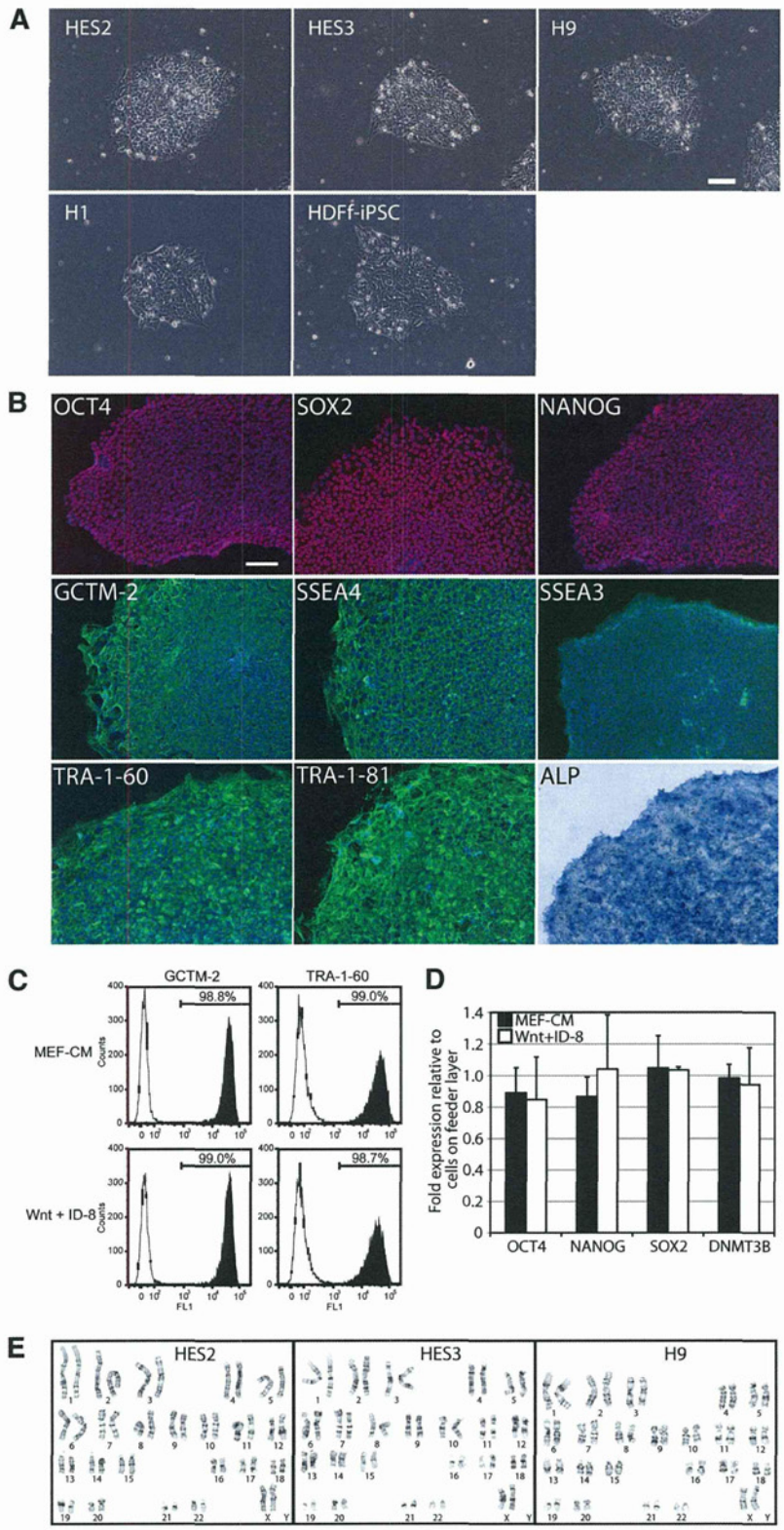

Figure 3. Characterization of human pluripotent cells maintained in xeno-free and feeder-free culture system. **(A):** Typical colony morphologies at passage 7. **(B):** Immunostaining of undifferentiated cell markers in HES3 cells at passage 24. Similar results were observed in H9 and HES2 cells (data not shown). **(C):** Flow cytometry analysis of undifferentiated cell markers in H9 cells at passage 26. White histograms indicate cells stained with secondary antibody; black histograms indicate cells stained with primary and secondary antibodies. Percentages of positive cells are listed on the bars. Similar results were observed in HES2 and HES3 cells (data not shown). **(D):** Quantitative polymerase chain reaction analysis of pluripotent stem cell markers in HES2 cells at passage 24. Error bars indicate SD. Similar results were observed in H9 and HES3 cells (data not shown). **(E):** G-banding karyotype at passage 22. Abbreviations: iPSC, induced pluripotent stem cell; MEF-CM, mouse embryonic fibroblast conditioned medium.

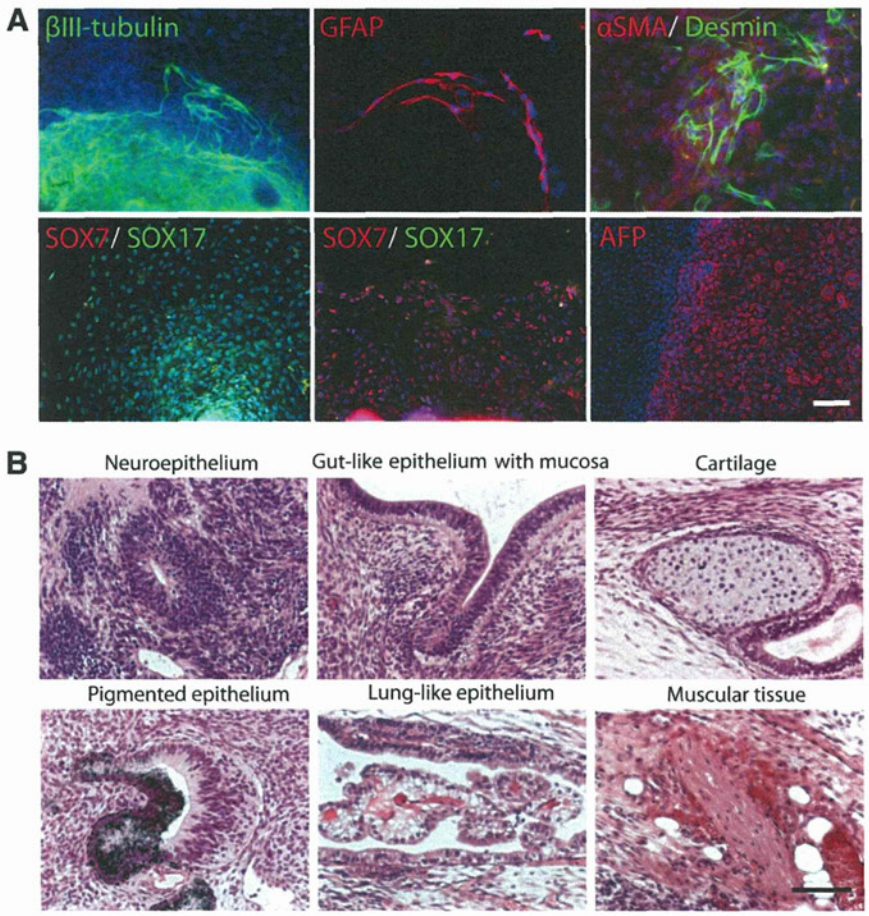

Figure 4. Differentiation capacity of human pluripotent stem cells maintained in xeno-free and feeder-free culture system. **(A):** Immunostaining of ectoderm (βIII-tubulin and GFAP), mesoderm (αSMA, Desmin), endoderm (AFP), definitive endoderm (SOX17-positive and SOX7-negative) and extraembryonic endoderm (SOX7-positive and SOX17-weakly positive)-derived cell markers from in vitro differentiation assay with HES3 cells after passages 17–24. Similar results were observed in the differentiation assay with H9 and HES2 cells (data not shown). **(B):** Ectodermal (neuroepithelium and pigmented cell), mesodermal (muscle and cartilage), and endodermal (gut-like and lung-like) tissue in teratoma formed with H9 cells after passage 22 in the culture system. Similar results were observed in teratomas from HES2 and HES3 cells (data not shown). Scale bars = 100 μm. Abbreviations: AFP, α-fetoprotein; GFAP, glial fibrillary acidic protein; SMA, smooth muscle actin.

several compounds reported to act as activators of the Wnt/β-catenin signaling pathway, we anticipate that these could be incorporated into the system we describe to further eliminate protein growth factor requirements.

Several reports have demonstrated a role for Wnt/β-catenin signaling in mESC self-renewal together with FGF/MEK pathway inhibitors in the absence of LIF and serum. Under these conditions, Wnt appears to function via the interaction of β-catenin and the Tcf3 transcriptional repressor, with abrogation of Tcf3 repressor function and recruitment of Tcf1 as a transcriptional activator to pluripotent gene promoters. However, direct Wnt/β-catenin activation per se is dispensable in mESCs in LIF-dependent culture [14–16]. Additionally, it was recently shown that β-catenin, through a Tcf-independent mechanism, reinforces Oct4 activity to maintain pluripotency [36], and Wnt in combination with LIF prevents mESC differentiation to epiblast stem cell (EpiSC) [37]. To date, our understanding of Wnt/β-catenin signaling in human pluripotent stem cells has remained highly controversial because of the unresolved basis for the dual function of Wnt/β-catenin signaling in pluripotency and differentiation. Sato et al. described positive if short-term effects of BIO, a known small molecule inhibitor of GSK-3, on both mESC and hESC maintenance, demonstrating a normal differentiation program capacity after withdrawal from these conditions [12], although there has been significant controversy regarding these findings [13, 26].

Our previous investigations demonstrated that a small molecule Wnt/β-catenin signaling modulator could maintain mESC proliferation and pluripotency for extended periods of time in LIF- and serum-independent culture by modulating β-catenin transcriptional coactivator usage from p300 to CBP [22, 24]. The small molecules we studied, IQ-1 and ID-8, were originally identified through a screen for maintenance of mESC pluripotency. Here we show that ID-8 binds DYRK family members. The target of ID-8 is completely different from the target of IQ-1, the PR72/130 subunit of PP2A; however, ID-8 also enhances the CBP/β-catenin interaction indirectly in hESCs, and in that regard, its effects are mechanistically similar to the effects of IQ-1 in mESCs. The mechanism of DYRK inhibition in hESCs by ID-8 was confirmed by the observation of a similar phenotype in DYRK knockdown and ID-8-treated hESCs. Therefore, the different effects of

IQ-1 and ID-8 in hESCs may be dependent on the differences in the function or expression of PR72/130 and DYRKs in mESCs and hESCs. The DYRK family is known to facilitate differentiation in many tissues and to interact with many proteins involved in stem cell proliferation and survival, including p53, STAT3, cyclin-D1, and caspase-9 [38–40]. However, their role in hESC self-renewal, differentiation, or Wnt/β-catenin signaling has not been previously reported. Further identification of DYRK substrates and the investigation of interaction between TCFs, CBP/p300, and DYRK in hESCs will be required to achieve a detailed understanding of the molecular mechanisms and of Wnt/β-catenin/TCF signaling in hESC self-renewal.

In the present study, we demonstrated long-term maintenance of pluripotency of hESCs in a Wnt/β-catenin/CBP-dependent fashion. Thus, a common plausible molecular mechanism for Wnt/β-catenin signaling maintaining in both mESC and hESC self-renewal is emerging, in which β-catenin by specifically interacting with the coactivator CBP maintains pluripotency [41]. The role of Tcf1/Tcf3, either interacting via β-catenin and CBP/p300 or independently, has not yet been determined and is the subject of ongoing investigations. In this report, we demonstrated that Wnt/β-catenin signaling together with a small molecule DYRK inhibitor is sufficient to maintain hESCs in the undifferentiated state. Furthermore, we show that β-catenin coactivator usage is shifted from p300 to CBP, similar to our previous report concerning mESCs using the small molecule IQ-1, which although interacting with a completely different molecular target, also biases CBP/β-catenin transcription to maintain pluripotency. In our culture system, bFGF signaling is dispensable and only enhances proliferation, and the dosage of bFGF required to achieve this effect is much lower than that used in other xeno- and feeder-free culture systems [10]. This is the first demonstration to our knowledge that hESC self-renewal can be maintained independently of exogenous activation of FGF or TGFβ signaling. Our findings suggest that the controversy surrounding the role of Wnt/β-catenin signaling in embryonic stem cells in previous reports may be due to initial biasing of CBP/β-catenin transcription, which also drives a negative feedback loop, thereby increasing the p300/β-catenin interaction. Furthermore, mixed results from concurrent activation of other signaling pathways, such as bFGF and/or TGFβ, may have also complicated previous interpretations. This situation is similar to the requirements for Wnt/β-catenin signaling in mESCs in LIF-dependent versus LIF-independent culture systems. The culture system we describe provides a powerful platform to explore these questions, as it relies on the activation of a relatively limited and very different set of signaling pathways compared with other systems described to date.

Conclusion

In conclusion, we have developed a simple human pluripotent stem cell culture system containing minimal growth factors Wnt and the small molecule DYRK inhibitor ID-8 that provides for stem cell renewal in the absence of bFGF and TGFβ/Nodal/Activin signaling. Additionally, we have developed a gentle subculture methodology that uses a synthetic disintegrin peptide. Our system still requires purified human ECM molecules, which can be certified for GMP; however, this need could be obviated with the development of chemically defined substrates. GMP manufacturing of hESCs or iPSCs using this culture system could be an important step toward future regenerative medical therapies. These findings also provide novel insights into the biochemical regulation of hESC self-renewal and new tools to probe the signaling pathways that control it.

Acknowledgments

We thank the Stem Cell Core facilities at Children's Hospital Los Angeles and at the University of Southern California for providing hESCs. Work at Kyoto University was supported by New Energy and Industrial Technology Development Organization (NEDO) Japan, Grant #P10027 Fundamental Technology Development for Promoting Industrial Application of Human Stem Cells. Work at the University of Southern California was supported by California Institute for Regenerative Medicine, New Cell Lines Grant #RL1-00667-1, New Technology for the Derivation of Human Pluripotent Stem Cell Lines for Clinical Use.

Author Contributions

K.H.: conception, design, experimentation, data analysis and interpretation, writing, final approval of manuscript; J.-L.T.: conception, design, experimentation, data analysis and interpretation, writing; S.Y. and C.N.: experimentation, data analysis; C.-L.H.: data analysis and interpretation; H.S., M.M., T.M., M.Y., and C.L.: provided research materials; N.N.: data analysis and interpretation, financial support; M.F.P.: data analysis and interpretation, writing, financial support; M.K.: conception, design, data analysis and interpretation, writing, financial support, final approval of manuscript.

Disclosure of Potential Conflicts of Interest

Kouichi Hasegawa and Michael Kahn both have equity positions in Cell Guidance Systems, Inc. Cell Guidance Systems, Inc., has licensed technology from University of Southern California related to this work.

References

1 Thomson JA, Itskovitz-Eldor J, Shapiro SS et al. Embryonic stem cell lines derived from human blastocysts. Science 1998;282:1145–1147.

2 Reubinoff BE, Pera MF, Fong CY et al. Embryonic stem cell lines from human blastocysts: somatic differentiation in vitro. Nat Biotechnol 2000;18:399–404.

3 Yu J, Vodyanik MA, Smuga-Otto K et al. Induced pluripotent stem cell lines derived from human somatic cells. Science 2007;318:1917–1920.

4 Takahashi K, Tanabe K, Ohnuki M et al. Induction of pluripotent stem cells from adult human fibroblasts by defined factors. Cell 2007;131:861–872.

5 Ludwig TE, Levenstein ME, Jones JM et al. Derivation of human embryonic stem cells in defined conditions. Nat Biotechnol 2006;24:185–187.

6 Lu J, Hou R, Booth CJ et al. Defined culture conditions of human embryonic stem cells. Proc Natl Acad Sci U S A 2006;103:5688–5693.

7 Yao S, Chen S, Clark J et al. Long-term self-renewal and directed differentiation of human embryonic stem cells in chemically defined conditions. Proc Natl Acad Sci U S A 2006;103:6907–6912.

8 Pera MF, Tam PP. Extrinsic regulation of pluripotent stem cells. Nature 2010;465:713–720.

9 Hasegawa K, Pomeroy JE, Pera MF. Current technology for the derivation of pluripotent stem cell lines from human embryos. Cell Stem Cell 2010;6:521–531.

10 Chen G, Gulbranson DR, Hou Z et al. Chemically defined conditions for human iPSC derivation and culture. Nat Methods 2011;8:424–429.

11 Komiya Y, Habas R. Wnt signal transduction pathways. Organogenesis 2008;4:68–75.

12 Sato N, Meijer L, Skaltsounis L et al. Maintenance of pluripotency in human and mouse embryonic stem cells through activation of Wnt signaling by a pharmacological GSK-3-specific inhibitor. Nat Med 2004;10: 55–63.

13 Dravid G, Ye Z, Hammond H et al. Defining the role of Wnt/β-catenin signaling in the survival, proliferation, and self-renewal of human embryonic stem cells. Stem Cells 2005;23: 1489–1501.

14 Lyashenko N, Winter M, Migliorini D et al. Differential requirement for the dual functions of beta-catenin in embryonic stem cell self-renewal and germ layer formation. Nat Cell Biol 2011;13:753–761.

15 Wray J, Kalkan T, Gomez-Lopez S et al. Inhibition of glycogen synthase kinase-3 alleviates Tcf3 repression of the pluripotency network and increases embryonic stem cell resistance to differentiation. Nat Cell Biol 2011;13: 838–845.

16 Yi F, Pereira L, Hoffman JA et al. Opposing effects of Tcf3 and Tcf1 control Wnt stimulation of embryonic stem cell self-renewal. Nat Cell Biol 2011;13:762–770.

17 Cai L, Ye Z, Zhou BY et al. Promoting human embryonic stem cell renewal or differentiation by modulating Wnt signal and culture conditions. Cell Res 2007;17:62–72.

18 Melchior K, Weiß J, Zaehres H et al. The WNT receptor FZD7 contributes to self-renewal signaling of human embryonic stem cells. Biol Chem 2008;389:897–903.

19 Sumi T, Tsuneyoshi N, Nakatsuji N et al. Defining early lineage specification of human embryonic stem cells by the orchestrated balance of canonical Wnt/β-catenin, Activin/Nodal and BMP signaling. Development 2008; 135:2969–2979.

20 Otero JJ, Fu W, Kan L et al. β-Catenin signaling is required for neural differentiation of embryonic stem cells. Development 2004; 131:3545–3557.

21 Emami KH, Nguyen C, Ma H et al. A small molecule inhibitor of beta-catenin/CREB-binding protein transcription [corrected]. Proc Natl Acad Sci U S A 2004;101: 12682–12687.

22 Miyabayashi T, Teo J-L, Yamamoto M et al. Wnt/β-catenin/CBP signaling maintains long-term murine embryonic stem cell pluripotency. Proc Natl Acad Sci U S A 2007;104:5668–5673.

23 Lukaszewicz AI, McMillan MK, Kahn M. Small molecules and stem cells. Potency and lineage commitment: The new quest for the fountain of youth. J Med Chem 2010;53:3439–3453.

24 Miyabayashi T, Yamamoto M, Sato A et al. Indole derivatives sustain embryonic stem cell self-renewal in long-term culture. Biosci Biotechnol Biochem 2008;72:1242–1248.

25 Hasegawa K, Zhang P, Wei Z et al. Comparison of reprogramming efficiency between transduction of reprogramming factors, cell-cell fusion, and cytoplast fusion. Stem Cells 2010;28:1338–1348.

26 Hasegawa K, Fujioka T, Nakamura Y et al. A method for the selection of human embryonic stem cell sublines with high replating efficiency after single-cell dissociation. Stem Cells 2006;24:2649–2660.

27 Willert K, Brown JD, Danenberg E et al. Wnt proteins are lipid-modified and can act as stem cell growth factors. Nature 2003;423:448–452.

28 Veeman MT, Slusarski DC, Kaykas A et al. Zebrafish prickle, a modulator of noncanonical Wnt/Fz signaling, regulates gastrulation movements. Curr Biol 2003;13:680–685.

29 Xu C, Inokuma MS, Denham J et al. Feeder-free growth of undifferentiated human embryonic stem cells. Nat Biotechnol 2001;19: 971–974.

30 Watanabe K, Ueno M, Kamiya D et al. A ROCK inhibitor permits survival of dissociated human embryonic stem cells. Nat Biotechnol 2007;25:681–686.

31 Chung TL, Turner JP, Thaker NY et al. Ascorbate promotes epigenetic activation of CD30 in human embryonic stem cells. Stem Cells 2010;28:1782–1793.

32 Ellerström C, Strehl R, Moya K et al. Derivation of a xeno-free human embryonic stem cell line. Stem Cells 2006;24:2170–2176.

33 Crook JM, Peura TT, Kravets L et al. The generation of six clinical-grade human embryonic stem cell lines. Cell Stem Cell 2007;1:490–494.

34 Desbordes SC, Placantonakis DG, Ciro A et al. High-throughput screening assay for the identification of compounds regulating self-renewal and differentiation in human embryonic stem cells. Cell Stem Cell 2008;2: 602–612.

35 Damoiseaux R, Sherman SP, Alva JA et al. Integrated chemical genomics reveals modifiers of survival in human embryonic stem cells. Stem Cells 2009;27:533–542.

36 Kelly KF, Ng DY, Jayakumaran G et al. β-Catenin enhances Oct-4 activity and reinforces pluripotency through a TCF-independent mechanism. Cell Stem Cell 2011;8:214–227.

37 Berge DT, Kurek D, Blauwkamp T et al. Embryonic stem cells require Wnt proteins to prevent differentiation to epiblast stem cells. Nat Cell Biol 2011;13:1070–1075.

38 Mercer SE, Friedman E. Mirk/Dyrk1B: a multifunctional dual-specificity kinase involved in growth arrest, differentiation, and cell survival. Cell Biochem Biophys 2006;45: 303–315.

39 Takahashi-Yanaga F, Sasaguri T. GSK-3beta regulates cyclin D1 expression: a new target for chemotherapy. Cell Signal 2008;20: 581–589.

40 Park J, Song W-J, Chung KC. Function and regulation of Dyrk1A: towards understanding Down syndrome. Cell Mol Life Sci 2009;66: 3235–3240.

41 Marson A, Foreman R, Chevalier B et al. Wnt signaling promotes reprogramming of somatic cells to pluripotency. Cell Stem Cell 2008; 3:132–135.

Wnt Signaling Orchestration with a Small Molecule DYRK Inhibitor Provides Long-Term Xeno-Free Human Pluripotent Cell Expansion

Kouichi Hasegawa, Shin-ya Yasuda, Jia-Ling Teo, Cu Nguyen, Michael McMillan, Chih-Lin Hsieh, Hirofumi Suemori, Norio Nakatsuji, Masashi Yamamoto, Tomoyuki Miyabayashi, Carolyn Lutzko, Martin F. Pera and Michael Kahn

Stem Cells Trans Med 2012;1;18-28; originally published online December 7, 2011; DOI: 10.5966/sctm.2011-0033

Journal of Cellular Physiology

Neutrophil Differentiation From Human-Induced Pluripotent Stem Cells

TATSUYA MORISHIMA,[1] KEN-ICHIRO WATANABE,[1] AKIRA NIWA,[2] HISANORI FUJINO,[1] HIROSHI MATSUBARA,[1] SOUICHI ADACHI,[1] HIROFUMI SUEMORI,[3] TATSUTOSHI NAKAHATA,[2] AND TOSHIO HEIKE[1]*

[1]*Department of Pediatrics, Graduate School of Medicine, Kyoto University, Kyoto, Japan*

[2]*Department of Clinical Application, Center for iPS Cell Research and Application, Kyoto University, Kyoto, Japan*

[3]*Laboratory of Embryonic Stem Cell Research, Stem Cell Research Center, Institute for Frontier Medical Sciences, Kyoto University, Kyoto, Japan*

Induced pluripotent stem (iPS) cells are of potential value not only for regenerative medicine, but also for disease investigation. The present study describes the development of a neutrophil differentiation system from human iPS cells (hiPSCs) and the analysis of neutrophil function and differentiation. The culture system used consisted of the transfer of hiPSCs onto OP9 cells and their culture with vascular endothelial growth factor (VEGF). After 10 days, TRA 1-85^{+}CD34^{+}VEGF receptor-2 (VEGFR-2)^{high} cells were sorted and co-cultured with OP9 cells in the presence of hematopoietic cytokines for 30 days. Floating cells were collected and subjected to morphological and functional analysis. These hiPSC-derived neutrophils were similar to peripheral blood mature neutrophils in morphology, contained functional neutrophil specific granules, and were equipped with the basic functions such as phagocytosis, superoxide production, and chemotaxis. In the process of differentiation, myeloid cells appeared sequentially from immature myeloblasts to mature segmented neutrophils. Expression patterns of surface antigen, transcription factors, and granule proteins during differentiation were also similar to those of granulopoiesis in normal bone marrow. In conclusion, differentiation of mature neutrophils from hiPSCs was successfully induced in a similar process to normal granulopoiesis using an OP9 co-culture system. This system may be applied to elucidate the pathogenesis of various hematological diseases that affect neutrophils.

J. Cell. Physiol. 226: 1283–1291, 2011.

Neutrophils and/or myeloid differentiation are most commonly affected in various hematological diseases including inherited bone marrow failure syndromes and neutrophil function disorders. Responsible genes have been identified in most of these syndromes or diseases, but the association between the gene mutation and the specific phenotype is not always clear. Moreover, often patients who present with a specific syndrome lack mutations in the known genes (Alter, 2007). Understanding the pathophysiology of these syndromes has been challenging despite the information provided by recent molecular findings, and in many of these syndromes, experimental models have not yet been generated.

Murine models of human congenital and acquired diseases are invaluable for disease investigation, but they provide a limited representation of human pathophysiology because they often do not faithfully mimic human diseases. The differences between murine and human physiologies make human cell culture an essential complement to research with animal models of disease.

Induced pluripotent stem (iPS) cells are reprogrammed somatic cells with embryonic stem (ES) cell-like characteristics generated by the introduction of combinations of specific transcription factors (Takahashi and Yamanaka, 2006; Meissner et al., 2007; Okita et al., 2007; Takahashi et al., 2007; Yu et al., 2007; Park et al., 2008b). Given the robustness of the approach, direct reprogramming promises to be a facile source of patient-derived cell lines. Such lines would be immediately valuable not only for regenerative medicine, but for disease investigation and drug screening as well.

The pluripotency and self-renewal potential of ES cells contributes to their value in various fields of science (Evans and Kaufman, 1981). Previous studies using normal or gene-manipulated ES cells have helped elucidate the process of normal embryogenesis and the genetic mechanisms of certain diseases (Lensch and Daley, 2006; Tulpule et al., 2010). Use of human embryos, however, faces ethical controversies that hinder the applications of human ES cells (hESCs). In addition, it is difficult to generate patient- or disease-specific ES cells, which are required for their effective application. The use of iPS cells would avoid the controversies surrounding human embryonic stem cell research.

Patient-specific iPS cells can be used for the generation of disease-corrected, patient-specific cells for cell therapy applications. Disease-specific pluripotent cells capable of differentiation into the various tissues affected in each condition can also provide new insights into disease pathophysiology by permitting analysis in a human system, under controlled conditions in vitro. Recent studies reported the generation of disease-specific iPS cell lines from patients with a variety of diseases (Park et al., 2008a; Raya et al., 2009; Agarwal et al., 2010). Therefore, disease-specific iPS cells are expected to be good models for the investigation of different diseases, and

Contract grant sponsor: The Ministry of Education, Culture, Sports, Science and Technology, Japan.

*Correspondence to: Toshio Heike, Department of Pediatrics, Graduate School of Medicine, Kyoto University, 54 Kawahara-cho, Shogoin, Sakyo-ku, Kyoto 606-8507, Japan.
E-mail: heike@kuhp.kyoto-u.ac.jp

Received 21 May 2010; Accepted 20 September 2010

Published online in Wiley Online Library (wileyonlinelibrary.com), 13 October 2010.
DOI: 10.1002/jcp.22456

effective neutrophil differentiation systems are required to investigate the pathogenesis of various hematological conditions that affect neutrophils using human iPS cells (hiPSCs).

Recent reports describe in vitro culture systems for neutrophil differentiation from hESCs (Choi et al., 2009; Saeki et al., 2009; Yokoyama et al., 2009); however, neutrophil differentiation from hiPSCs has not yet been reported in detail. One of these studies demonstrated that myeloid differentiation could be induced from hiPSCs using the same methodology employed for their differentiation from hESCs (Choi et al., 2009), but the differentiation process and the functions of hiPSC-derived neutrophils were not shown in detail. A system for erythroid differentiation from primate ES and murine iPS cells by co-culture with OP9 stromal cells was developed in previous studies (Umeda et al., 2004; Umeda et al., 2006; Shinoda et al., 2007; Niwa et al., 2009). In the present study, a neutrophil differentiation system from hiPSCs was established by modifying the erythroid differentiation system, and the functions of the hiPSC-derived neutrophils and their differentiation process were analyzed in detail. This system may contribute to the elucidation of the pathogenesis of various blood diseases and the development of novel therapeutic approaches.

Materials and Methods

Maintenance of cells

The human iPS cell lines 201B6, 253G1 and 253G4 were a kind gift from Dr. Yamanaka (Kyoto University, Kyoto), and were generated from human dermal fibroblasts by retrovirus-mediated transfection of four (201B6) or three (253G1 and 253G4) transcription factors (Oct3/4, Sox2, and Klf4, with or without c-Myc) (Takahashi et al., 2007; Nakagawa et al., 2008). The human iPS cell lines and the human ES cell line KhES3-EGFPneo (KhES-3G) were maintained on mitomycin-C (Kyowa Hakko Kirin, Tokyo, Japan) -treated mouse embryonic fibroblasts (MEFs) in DMEM/F12 (Sigma-Aldrich, St. Louis, MO) supplemented with 20% Knockout™ Serum Replacement (Invitrogen, Carlsbad, CA), 5 ng/ml basic fibroblast growth factor (bFGF; R&D Systems, Minneapolis, MN), 1% non-essential amino acids solution (Invitrogen), 5 mM sodium hydroxide solution, 100 μM 2-mercaptethanol, and 2 mM L-glutamine. The culture medium was replaced daily with fresh medium. Colonies were passaged onto new MEFs every 3 or 4 days. The human ES cell line was used in conformity with The Guidelines for Derivation and Utilization of Human Embryonic Stem Cells of the Ministry of Education, Culture, Sports, Science, and Technology, Japan. OP9 stromal cells, which were a kind gift from Dr. Kodama (Osaka University, Osaka), were maintained in α-MEM (Invitrogen) supplemented with 20% fetal calf serum (FCS; Biological Industries, Bet Haemek, Israel).

Antibodies

The antibodies used for flow cytometric analysis included fluorescein isothiocyanate (FITC)-conjugated anti-human TRA 1-85 (R&D Systems), CD45 (Becton-Dickinson, Franklin Lakes, NJ) antibodies, phycoerythrin (PE)-conjugated anti-human CD11b, CD34 (Beckman Coulter, Fullerton, CA), CD13, CD16, CD33 (Becton-Dickinson) antibodies, and allophycocyanin (APC)-conjugated anti-human vascular endothelial growth factor receptor-2 (VEGFR-2) (eBioscience, San Diego, CA) antibody. The primary antibodies used for immunocytochemical analysis included goat anti-human lactoferrin (Santa Cruz Biotechnology, Santa Cruz, CA) and rabbit anti-human MMP9 (Abcam, Cambridge, UK). Biotinylated horse anti-goat or anti-rabbit antibodies (Vector Laboratories, Burlingame, CA) were used as secondary antibodies.

Differentiation of iPS cells

Methods used for the initial differentiation of iPS cells and cell sorting were based on earlier reports (Umeda et al., 2004, 2006). Briefly, trypsin-treated undifferentiated iPS cells were transferred onto OP9 cells and cultured with 20 ng/ml vascular endothelial growth factor (VEGF) (R&D Systems). After 10 days, the induced cells were harvested with cell dissociation buffer (Invitrogen), and sorted TRA 1-85^{+}CD34^{+}VEGFR-2^{high} cells were transferred onto fresh OP9 cells in six-well plates at a concentration of 3×10^3 cells per well. Sorted cells were cultured in α-MEM (Invitrogen) containing 10% FCS (Sigma, St Louis, MO), 50 μM 2-mercaptoethanol, 20 ng/ml interleukin (IL)-3, 100 ng/ml stem cell factor (SCF) (R&D Systems), and 10 ng/ml thrombopoietin (TPO) for 20 days. On day 20 after cell sorting, cytokines were changed into 20 ng/ml IL-3 and 10 ng/ml granulocyte colony-stimulating factor (G-CSF). IL-3, TPO and G-CSF were kindly provided by Kyowa Hakko Kirin.

Flow cytometric analysis and cell sorting

Cells were trypsinized and stained with antibodies. Dead cells were excluded by 4',6-diamidino-2-phenylindole (DAPI) staining. Samples were analyzed using an LSR flow cytometer and Cell Quest software (Becton Dickinson). Cell sorting was performed using a FACSVantage SE flow cytometer (Becton Dickinson).

Cytostaining

Floating cells were centrifuged onto glass slides using a Shandon Cytospin® 4 Cytocentrifuge (Thermo, Pittsburgh, PA), and analyzed by microscopy after May–Giemsa, myeloperoxidase (MPO), or alkaline-phosphatase staining. Sequential morphological analysis was performed as follows: all adherent cells including OP9 cells were trypsinized, harvested, and incubated in a new tissue-culture dish (Becton-Dickinson) for 1 h to eliminate adherent OP9 cells (Suwabe et al., 1998). Floating cells were then collected, centrifuged onto glass slides, and analyzed by microscopy after May–Giemsa staining. For immunocytochemical analysis, cells were fixed with 4% paraformaldehyde (PFA), immersed in citrate buffer, and autoclaved for 5 min at 121°C for antigen retrieval (Toda et al., 1999). The slides were then incubated with primary antibodies followed by application of the streptavidinbiotin complex immunoperoxidase technique with diaminobenzidine as chromogen, and nuclei were counterstained with hematoxylin.

Electron microscopy

Cells were fixed in 2% glutaraldehyde in 0.1 M phosphate buffer (PB) for at least 2 h, and then postfixed in 1% osmium tetroxide in 0.1 M PB for 1.5 h. After fixation, samples were dehydrated in a graded ethanol series, cleared with propylene oxide, and embedded in Epon. Thin sections of cured samples were stained with uranyl acetate and Reynolds lead citrate. The sections were inspected using a transmission electron microscope, H7650 (Hitachi, Tokyo, Japan).

Chemotaxis assay

Chemotactic ability was determined using a modified Boyden chamber method (Boyden, 1962; Harvath et al., 1980). Briefly, 500 μl of the reaction medium (Hank's Balanced Salt Solution (HBSS) containing 2.5% FCS) with or without 10 nM formyl-Met-Leu-Phe (fMLP; Sigma-Aldrich) was placed into each well of a 24-well plate, and the cell culture insert (3.0-μm pores; Becton Dickinson) was gently placed into each well to divide the well into upper and lower sections. Floating cells were suspended in the reaction medium at 7.0×10^4/ml, and a 500-μl cell suspension was added to the upper well, allowing the cells to migrate from the upper to the lower side of the membrane for 4 h at 37°C. After incubation, cells in the lower chamber were collected and counted using an LSR flow cytometer. Cells were counted by flow cytometry as follows:

equivalent amounts of counting beads were added to each sample and counted until the bead count reached 10,000.

MPO activity assay

The EnzChek Myeloperoxidase (MPO) Activity Assay Kit (Molecular Probes, Leiden, The Netherlands) was used for rapid and sensitive determination of MPO chlorination activity in cell lysates. The procedure was performed following the manufacturer's instructions. Cell lysate samples were prepared from 1×10^4 floating cells by freeze-thaw cycles. Fluorescence was measured with a fluorescence microplate reader (Wallac 1420 ARVO sx; PerkinElmer, Waltham, MA) using fluorescence excitation and emission at 485 and 530 nm, respectively. The background fluorescence measured for each zero-MPO control reaction was subtracted from each fluorescence measurement before plotting.

DHR assay

Neutrophil production of reactive oxygen species was detected by flow cytometry using dihydrorhodamine123 (DHR) as described previously (Vowells et al., 1995). Briefly, 3.5×10^4 floating cells were suspended in 100 μl of the reaction buffer (HBSS containing 0.1% FCS and 5 mM glucose) per tube, and two tubes were prepared for each sample. Catalase (Sigma-Aldrich) at a final concentration of 1000 U/ml and DHR at a final concentration of 1.0×10^5 nM were added and incubated for 5 min in a 37°C shaking water bath. After incubation, phorbol myristate acetate (PMA; Sigma-Aldrich) at a final concentration of 400 ng/ml was added to one of the two tubes and tubes were returned to the water bath for an additional 15 min. Following incubation, rhodamine fluorescence from the oxidized DHR was detected using an LSR flow cytometer.

Phagocytosis and detection of reactive oxygen species

Phagocytosis and neutrophil production of reactive oxygen species was detected by chemiluminescent microspheres (luminol-binding carboxyl hydrophilic microspheres; TORAY, Tokyo, Japan) as described previously (Uchida et al., 1985). Briefly, 2×10^4 floating cells were suspended in 50 μl of the reaction buffer (HBSS containing 20 mM N-2-hydroxyethylpiperazine-N′-2-ethanesulfonic acid (HEPES)) per tube. To activate the system, 5 μl of chemiluminescent microspheres was added, and light emission was recorded continuously. During the measurement, samples were kept at 37°C. To inhibit the phagocytosis, 1.75 μg of cytochalasin B (Sigma-Aldrich) was added to the sample. Chemiluminescence from the microspheres was detected using a luminometer (TD-20/20; Turner Designs, Sunnyvale, CA).

RNA extraction and RT-PCR analysis

RNA samples were prepared using silica gel membrane-based spin-columns (RNeasy Mini-Kit™, Qiagen, Valencia, CA) and subjected to reverse transcription (RT) with the Ominscript-RT Kit™ (Qiagen). All procedures were performed following the manufacturer's instructions. For reverse transcriptase-polymerase chain reaction (RT-PCR), yields were adjusted by dilution to produce equal amounts of the human glyceraldehyde-3-phosphate dehydrogenase (GAPDH) amplicon. The complementary DNA (cDNA) templates were initially denatured at 94°C for 5 min, followed by 30–40 amplification reactions consisting of 94°C for 15–30 sec (denaturing), 55–63°C for 15–30 sec (annealing), and 72°C for 30–60 sec (extension), with a final extension at 72°C for 7 min. The oligonucleotide primers were as follows: NANOG, 5′-CAG CCC TGA TTC TTC CAC CAG TCC C-3′ and 5′-TGG AAG GTT CCC AGT CGG GTT CAC C-3′ (Takahashi et al., 2007); human GAPDH, 5′-CAC CAG GGC TGC TTT TAA CTC TG-3′ and 5′-ATG GTT CAC ACC CAT GAC GAA C-3′ (Umeda et al., 2006); PU.1, 5′-CTG CAT TGG CCC CCA CCG AG-3′ and 5′-AGG TCT TCT GAT GGC TGA GGG GG-3′; C/EBPα, 5′-TAA CCT TGT GCC TTG GAA ATG CAA AC-3′ and 5′- ATG TTT CCA CCC CTT TCT AAG GAC A-3′ (Duan and Horwitz, 2003); C/EBPε, 5′- AGT CTG GGG AAG AGC AGC TTC-3′ and 5′- ACA GTG TGC CAC TTG GTA CTG-3′ (Mori et al., 2009); MPO, 5′-TGA GGA CGG CTT CTC TCT TC-3′ and 5′-CCC GGT AAG TGA TGA TCT GG-3′; Lactoferrin, 5′-AGC TGG CAG ACT TTG CGC T-3′ and 5′-TTC AGA TTA GTA ATG CCT GCG ACA TAC-3′ (Kholodnyuk et al., 2006); Gelatinase (MMP-9), 5′-GCC TCC AAC CAC CAC CAC AC-3′ and 5′-GCC CAG CCC ACC TCC ACT C-3′ (Sugimoto et al., 2001); mouse GAPDH, 5′-ACG GCC GCA TCT TCT TGT GCA-3′ and 5′-CAC CCT TCA AGT GGG CCC CG-3′. PCR amplification reaction cycles were performed in the linear range for each primer by carrying out primer titrations. The number of reaction cycles per sample were: NANOG, 35 cycles; human GAPDH, 30 cycles; PU.1, 40 cycles; C/EBPα, 40 cycles; C/EBPε, 40 cycles; MPO, 35 cycles; Lactoferrin, 35 cycles; Gelatinase (MMP-9), 40 cycles; mouse GAPDH, 30 cycles.

Statistics

Statistical analyses were conducted using the Student's *t*-test. Statistical significance was defined as $P < 0.05$.

Results

Neutrophil differentiation from hiPSCs in co-culture with OP9 stromal cells

A culture system for the induction of erythroid cell differentiation from primate ES and murine iPS cells by co-culture with OP9 stromal cells (Umeda et al., 2004; Umeda et al., 2006; Shinoda et al., 2007; Niwa et al., 2009) was established, and this system was applied for neutrophil differentiation from hiPSCs. Prior data in primate ES cells suggested that the VEGFR-2^{high} fraction of differentiated cells contained hemangioblasts and VEGFR-2^{high}CD34$^+$ cells had more hematopoietic potential (Umeda et al., 2006). Therefore, the expression of VEGFR-2 and CD34 was examined using three human iPS cell lines (201B6, 253G1, 253G4) and one ES cell line (KhES-3G). After 10 days of co-culture with OP9 in the presence of 20 ng/ml VEGF, VEGFR-2^{high}CD34$^+$ cells appeared from all hiPSC lines in a similar manner to the ES cell line (Fig. 1A). Among these three human iPS cell lines, the highest percentage of VEGFR-2^{high}CD34$^+$ cells was detected in 253G4 (Fig. 1B), and the data on this cell line is therefore presented below.

The VEGFR-2^{high}CD34$^+$ cell fraction was sorted (Fig. 1C) and 1.1×10^4 (range; $0.6–2.2 \times 10^4$ in 14 independent cultures) VEGFR-2^{high}CD34$^+$ cells were grown in one 10-cm dish containing hiPSCs. They were then transferred onto fresh OP9 cells and cultured in the presence of hematopoietic cytokines. Around 10 days after cell sorting (day10 + 10), small, round cell colonies appeared (Fig. 1D), and these colonies gradually grew in both size and number (Fig. 1E). At the same time, floating cells also appeared, and the average number of floating cells from 1×10^4 sorted VEGFR-2^{high}CD34$^+$ cells at 30 days after cell sorting (day10 + 30) was 4.1×10^4 (range; $0.2–9.9 \times 10^4$ in 11 independent cultures).

May–Giemsa staining of the floating cells on day 10 + 30 revealed that 38.0 ± 1.6% of the cells were stab and segmented neutrophils (Fig. 1F), which were positive for MPO (Fig. 1G) and neutrophil alkaline-phosphatase (Fig. 1H). The rest were mainly immature myeloid cells and a small number of macrophages, and cells of other lineages, such as erythroid or lymphoid cells, were not observed. The frequency of MPO- and neutrophil alkaline-phosphatase-positive cells is shown in Table 1. The results were consistent with the morphological features revealed by May–Giemsa staining.

Surface marker analysis revealed that these floating cells were positive for CD45 and CD11b, and partially positive for CD13, CD33, and CD16 (Fig. 1I). The expression pattern of these surface markers was similar to that of neutrophils or immature myeloid cells in healthy bone marrow (van Lochem et al., 2004), although the CD16 expression level was lower.

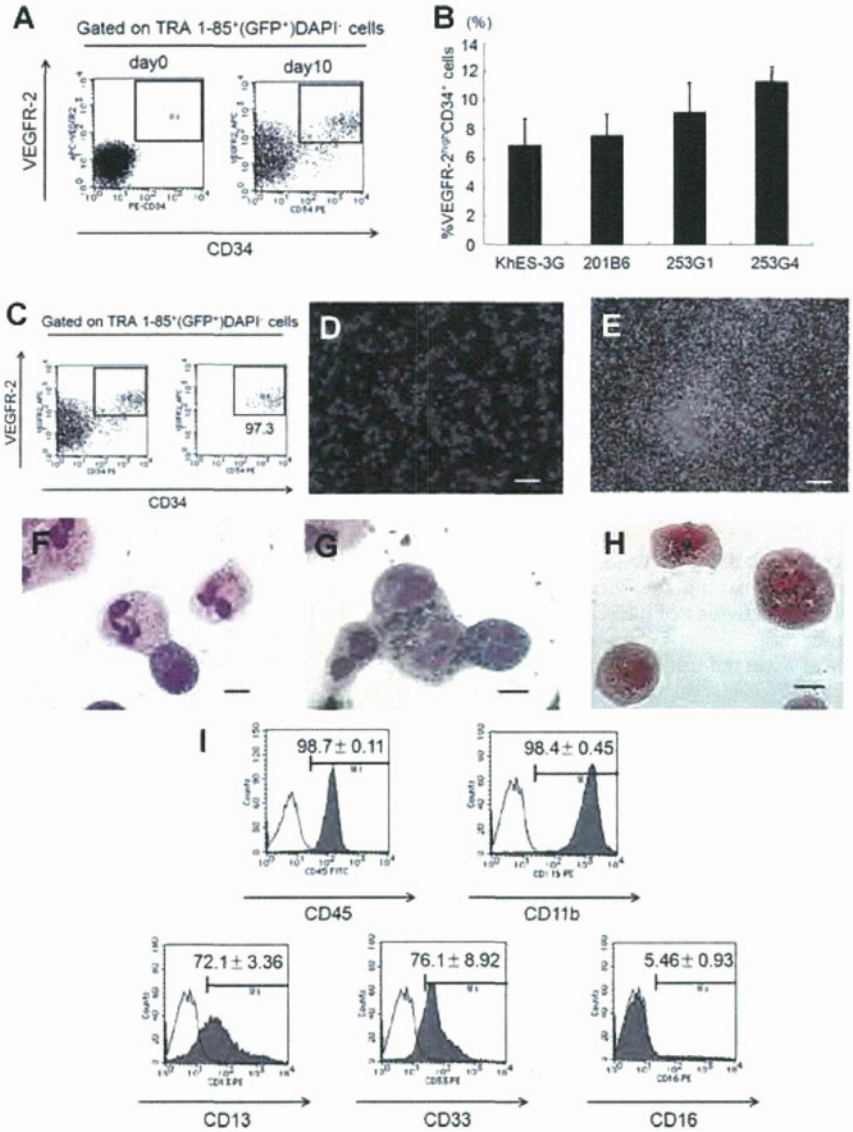

Fig. 1. Neutrophil differentiation from hiPSCs in co-culture with OP9 stromal cells. (A–B) Flow cytometric analysis of VEGFR-2 and CD34 during differentiation induction. TRA 1-85$^+$ (GFP$^+$) DAPI$^-$ cells were gated as human iPS (ES) cell-derived viable cells. Undifferentiated iPS (ES) cells and 10-day culture cells were stained with antibodies specific for VEGFR-2 and CD34. Representative results from one of three independent experiments (A) and percentages of VEGFR-2^{high}CD34$^+$ cells on day 10 (B) are shown (n = 3; bars represent SDs). (C) VEGFR-2^{high}CD34$^+$ cells were sorted on day 10. Representative dot plots and percentages of gated cells are shown. Purities of viable VEGFR-2^{high}CD34$^+$ cells were calculated at 95.5 ± 1.9% from 14 independent experiments. (D–E) Micrographs of adherent hematopoietic cell clusters generated on day 10 (D) and day 30 (E) after cell sorting. Scale bars: 200 μm. (F–H) May–Giemsa staining (F), myeloperoxidase staining (G), and neutrophil alkaline-phosphatase staining (H) of floating cells on day 10 + 30. Scale bars: 10 μm. (I) Flow cytometric analysis of floating cells on day 10 + 30 were stained with antibodies specific for CD45, CD11b, CD13, CD33, or CD16. Plots show the negative control profile (open bars) versus the specific antibody staining profiles (shaded bars). Representative results from one of three independent experiments are shown. [Color figure can be viewed in the online issue, which is available at wileyonlinelibrary.com.]

TABLE 1. Frequency of staining-positive cells for neutrophil specific granules

Staining	Frequency of positive cells (%)
Myeloperoxidase	93.7 ± 1.7
Neutrophil alkaline-phosphatase	39.0 ± 2.2
Lactoferrin	79.0 ± 1.4
Gelatinase	59.0 ± 3.7

Data are shown as mean ± SD (n = 3 independent experiments).

This lower CD16 expression level was similar to that of neutrophils derived in vitro from bone marrow CD34$^+$ cells by stimulation with G-CSF (Kerst et al., 1993b) and to the effect in vivo when G-CSF is administered to healthy volunteers (Kerst et al., 1993a). These results indicated that the modified OP9 co-culture system could differentiate mature neutrophils from immature hiPSCs.

hiPSC-derived neutrophils contain neutrophil specific granules

Mature neutrophils in vivo have intracellular granules that are important for their bactericidal function. The granules can be

classified into three types based on their size, morphology, or electron density, or with reference to a given protein: primary (azurophilic) granules contain MPO, secondary granules contain lactoferrin, and tertiary granules contain gelatinase (Borregaard and Cowland, 1997).

To assess the presence of these granules in hiPSC-derived neutrophils, they were imaged using transmission electron microscopy, which showed that the hiPSC-derived mature neutrophils contained peroxidase-positive and negative granules, as was observed in peripheral blood neutrophils (Fig. 2A–B). Immunocytochemical analysis revealed that hiPSC-derived mature neutrophils were also positive for lactoferrin and gelatinase (Fig. 2C–D). The frequencies of cells that were positive for neutrophil specific granules, as observed by transmission electron microscopy (Table 2) and immunocytochemical analysis (Table 1), were more than 90% for primary granules, about 80% for secondary granules, and approximately 60% for tertiary granules. These results indicated that hiPSC-derived neutrophils contained neutrophils-specific granules.

hiPSC-derived neutrophils exhibit biological bactericidal activities

Because neutrophils patrol circulating blood and play a key role in early phase defense mechanisms, the chemotactic, phagocytotic, and bactericidal activities of hiPSC-derived neutrophils were analyzed.

Chemotactic activity was assessed using a modified Boyden chamber method (Boyden, 1962; Harvath et al., 1980). After incubation with or without fMLP in the lower well, neutrophils had migrated from the upper side to the lower side of the membrane. Incubation with fMLP caused an increase in the number of migrated cells of more than three times compared to cells without fMLP, suggesting that hiPSC-derived neutrophils had chemotactic activity in response to a chemoattractant similar to natural neutrophils derived from bone marrow (Fig. 3A).

The MPO-dependent chlorination activity and reactive oxygen production of hiPSC-derived neutrophils, which are

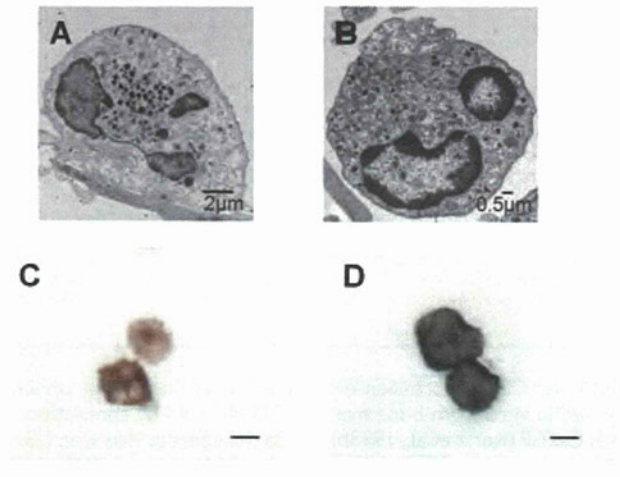

Fig. 2. Neutrophil-specific granules in hiPSC-derived neutrophils. (A–B) Floating cells on day10 + 30 (A) and peripheral blood neutrophils (B) were analyzed by transmission electron microscope. (C–D) Immunocytochemical analysis. Floating cells on day10 + 30 were stained for lactoferrin (C) and MMP9 (gelatinase) (D). Scale bars: 10 μm. [Color figure can be viewed in the online issue, which is available at wileyonlinelibrary.com.]

TABLE 2. Frequency of positive cells for neutrophil specific granules under transmission electron microscopy

Granules	Frequency of positive cells (%)
Peroxidase-positive granules	95.1 (135/142)
Peroxidase-negative granules	86.6 (123/142)

both essential for their bactericidal function, were determined next. MPO reacts with hydrogen peroxide (H_2O_2) to form the active redox and enzyme intermediate compound MPO-I, which oxidizes chloride (Cl^-) to HOCl (Winterbourn, 2002). As shown in Figure 3B, hiPSC-derived neutrophils showed MPO-dependent chlorination activity. To evaluate reactive oxygen production, the ability to convert DHR to rhodamine was assessed using flow cytometry (Vowells et al., 1995) and the results revealed that hiPSC-derived neutrophils characteristically produced superoxide in response to PMA (Fig. 3C).

Finally, phagocytotic activity and phagosome-dependent reactive oxygen production were measured using luminol-bound microspheres (Uchida et al., 1985). As shown in Figure 3D, the captured data confirmed that hiPSC-derived neutrophils could produce reactive oxygen species in response to the phagocytosis of microspheres, which was completely abolished in the presence of the antiphagocytic agent cytochalasin B. Moreover, transmission electron microscopy successfully captured a screenshot of a neutrophil phagocytosing the microbeads (Fig. 3E). The above results clearly show that neutrophils derived from hiPSC using the present culture system maintain their functional status.

Step-wise neutrophil differentiation from hiPSCs is similar to normal granulopoiesis

Disorders of neutrophil differentiation are observed in various hematological diseases, among them the maturation arrest of neutrophil precursors in the bone marrow at the promyelocyte stage in severe congenital neutropenia. Thus, in clinical applications for disease investigation, the sequential analysis of the differentiation process from hiPSC to mature neutrophils in this culture system is required.

Observation of the sequential changes in cell morphology was done using May–Giemsa staining. Visualization of the morphology of day10 + 10 cells revealed that the cells were mainly myeloblasts and promyelocytes (Fig. 4A). On day10 + 20, myelocytes and metamyelocytes became predominant (Fig. 4B), and on day 10 + 30, stab and segmented neutrophils became predominant (Fig. 4C).

Surface antigen expression at each differentiation stage of hiPSC-derived cells was analyzed by flow cytometry (Fig. 4D). CD34, cell surface marker on normal immature hematopoietic cells, was detected in about 20% of the cells on day 10 + 10, but disappeared gradually thereafter. From day 10 + 10 to 10 + 30, the common myeloid antigens CD11b and CD33 were expressed in almost all the cells. Interestingly, expression of CD13, also a common myeloid antigen, was observed in less than 20% of cells at day 10 + 10 and did not subsequently increase. The expression level of CD16, which is a representative marker of matured neutrophils (van de Winkel and Anderson, 1991), doubled from day 10 + 10 to day 10 + 20, although the increase in expression was not statistically significant. These expression patterns were consistent with the patterns observed during normal neutrophil differentiation in healthy bone marrow (van Lochem et al., 2004).

The gene expression patterns of the pluripotency marker, transcription factors and granule proteins during neutrophil

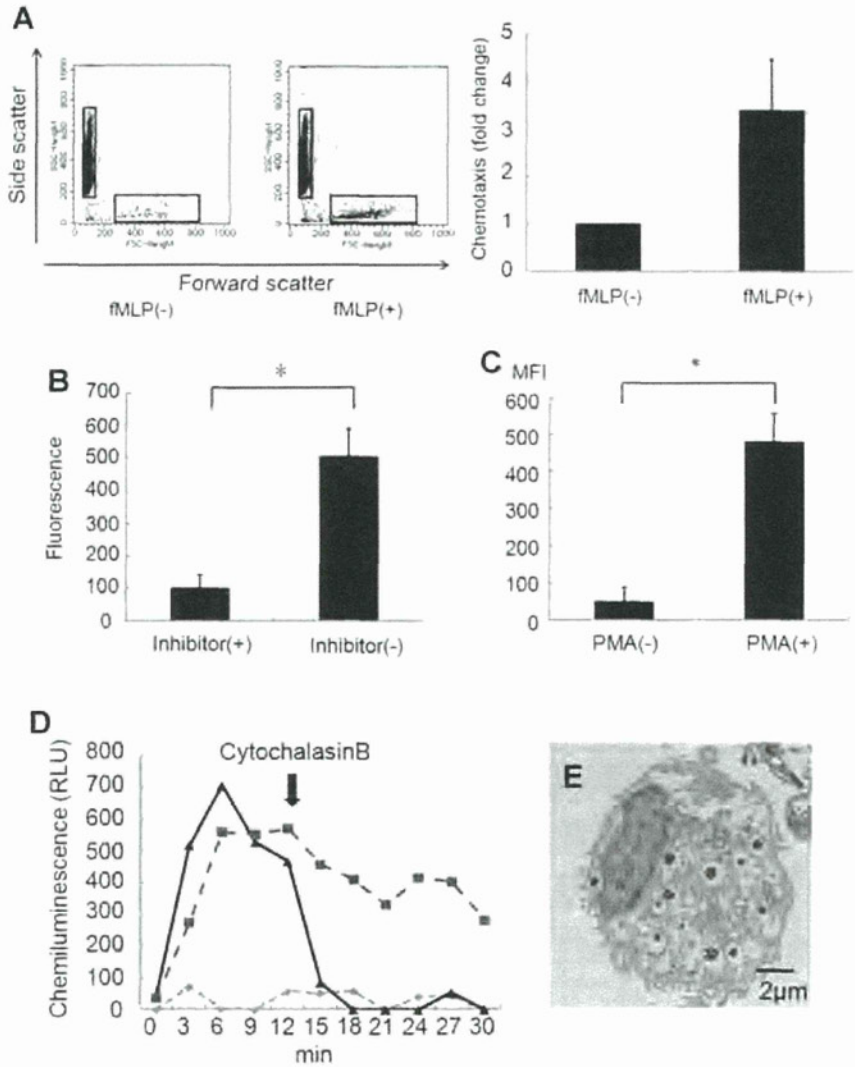

Fig. 3. Functional analysis of hiPSC-derived neutrophils. (A) Chemotactic activity of floating cells on day10 + 30 in response to fMLP was determined as described in Materials and Methods section. After a 4-h culture, the transwell inserts were removed, and the cells in the lower chamber were counted by an LSR flow cytometer (n = 3; bars represent SDs). (B) MPO chlorination activity in cell lysates from floating cells on day10 + 30 was analyzed by EnzChek Myeloperoxidase (MPO) Activity Assay Kit as described in the Materials and Methods section. The chlorination activity in neutrophil cell lysates was almost completely abolished by the addition of a chlorination inhibitor (n = 3; bars represent SDs; *P < 0.05.). (C) Floating cells on day10 + 30 were subjected to DHR assay. DHR was reacted with neutrophils with or without PMA, and the resultant rhodamine fluorescence was detected by flow cytometry. The addition of PMA increased the levels of fluorescence. Results are expressed as mean fluorescence intensity (MFI) (n = 3; bars represent SDs; *P < 0.05.). (D) Floating cells on day10 + 30 were subjected to the assay for phagocytosis-induced respiratory burst activity using chemiluminescent microspheres (luminol-binding microspheres). Gradual increase in chemiluminescence indicates the respiratory burst triggered by the phagocytosis of luminol-binding microspheres (squares). The increase in chemiluminescence was almost completely abolished by the addition of cytochalasin B (diamonds) and inhibited by its later addition (triangles). The figures are representative of three independent experiments. Abbreviation: RLU, relative light units. (E) hiPSC-derived neutrophils phagocytosing the microbeads were analyzed by transmission electron microscopy.

differentiation in this culture system were investigated by RT-PCR (Fig. 4E–F). NANOG, a pluripotency marker, was expressed in undifferentiated iPS cells but disappeared in sorted VEGFR2^{high}CD34^{+} cells after 10 days differentiation. PU.1 and C/EBPα, essential transcription factors for commitment and differentiation of the granulocytic lineage (Borregaard et al., 2001; Friedman, 2007) were first detected on day 10 + 10 and persisted thereafter. C/EBPε, which had a critical role for the later stages of neutrophil development and transcription of key granule proteins (Borregaard et al., 2001; Friedman, 2007) were first detected faintly on day 10 + 10 and upregulated thereafter. MPO and lactoferrin, which were expressed at the highest levels in myeloblasts/promyelocytes and myelocytes/metamyelocytes, respectively (Cowland and Borregaard, 1999; Borregaard et al., 2001), were detected on day 10 + 10. Gelatinase, which was expressed at the highest level in band and segmented neutrophilic cells (Cowland and Borregaard, 1999; Borregaard et al., 2001), was first detected on day 10 + 20 and upregulated thereafter. Altogether, these results suggested that the neutrophil differentiation in this co-culture system might recapitulate the orderly differentiation process in bone marrow.

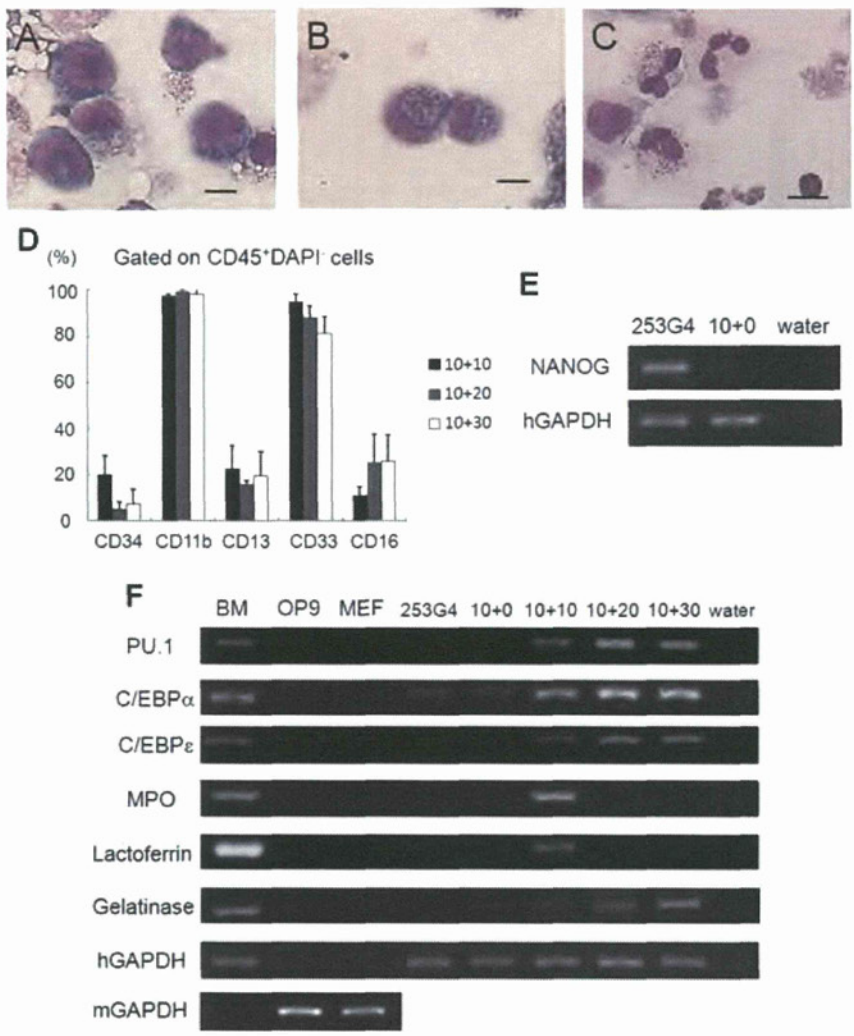

Fig. 4. Sequential analysis of neutrophil differentiation from hiPSCs. (A–C) Sequential morphological analysis of day 10 + 10 (A), day 10 + 20 (B) and day 10 + 30 (C). Scale bars: 10 μm. (D) Surface antigen expression at each level of differentiation of hiPSC-derived cells was analyzed by flow cytometry. All adherent cells including OP9 cells were harvested and stained with antibodies. Human $CD45^{+}DAPI^{-}$ cells were gated as hiPSC-derived viable leukocytes (n = 3; bars represent SDs). (E–F) Sequential RT-PCR analysis of a pluripotency marker (E), genes associated with neutrophil development and neutrophils-specific granules (F) during differentiation. Human GAPDH was used as a loading control. Abbreviations: BM, human bone marrow cells; 253G4, undifferentiated 253G4 cells; 10 + 0, sorted $VEGFR2^{high}CD34^{+}$ cells after 10 days differentiation; 10 + 10, 20, 30, all cells after 10, 20, 30 days differentiation after cell sorting; hGAPDH, human GAPDH; mGAPDH, mouse GAPDH. The figures are representative of three independent experiments. [Color figure can be viewed in the online issue, which is available at wileyonlinelibrary.com.]

Discussion

The analysis of the differentiation process of neutrophils can provide helpful information for the elucidation of the pathogenesis of hematopoietic diseases that affect neutrophils and/or myeloid differentiation, including inherited bone marrow failure syndromes and neutrophil function disorders. Traditionally, HL-60, an acute promyelocytic cell line, has been used as a neutrophil differentiation model (Collins et al., 1978; Newburger et al., 1979). Although this cell line grows well and differentiates easily into neutrophils, the neutrophil differentiation model is not suitable for the analysis of neutrophil-affected disorders because of its leukemic cell-origin. Development of a neutrophil differentiation system based on iPS cells would provide a better model for the analysis of such diseases, because iPS cells can be generated from the somatic cells of patients suffering from these diseases.

The current study aimed to investigate two issues in hiPSC-derived neutrophil differentiation: tracking the step-wise maturation in vitro and evaluating the wide spectrum of neutrophil functions. Through the use of a modified OP9 co-culture system, the directed and step-wise differentiation from hiPSCs to mature neutrophils containing neutrophil specific granules was first accomplished. The expression of surface antigens, transcription factors and granule proteins during differentiation exhibited the characteristic pattern of normal granulopoiesis. The biological functions of hiPSC-derived neutrophils were demonstrated through the quantitative assessment of granule enzyme activities and biological bactericidal activities such as chemotaxis and phagocytosis.

Defects in the maturation and function of neutrophils are associated with certain blood diseases including inherited bone marrow failure syndromes and neutrophil function disorders.

Among bone marrow failure syndromes, certain conditions affect a specific maturation stage, such as the maturation arrest at the plomyelocyte/myelocyte stage seen in severe congenital neutropenia. Neutrophil function disorders can affect specific bactericidal activities, such as the absence of MPO activity characteristic of MPO deficiency disorders. The use of hiPSCs for the investigation of these diseases requires sequential analyses that can identify each neutrophil maturation stage and include a functional analysis to evaluate each bactericidal activity separately on disease-specific, iPSC-derived neutrophils. Although previous studies have reported neutrophil differentiation models from hESCs (Choi et al., 2009; Saeki et al., 2009; Yokoyama et al., 2009) and hiPSC-derived neutrophils have been shown before (Choi et al., 2009), evidence showing that hiPSCs, which are artificially reprogrammed somatic cells, can follow the normal developmental pathway into fully functional mature neutrophils is of great significance, and the description of methods for identifying each neutrophil maturation step and analyzing each bactericidal pathway separately is important for clinical applications.

Although flow-cytometric analysis combined with RT-PCR identified the neutrophil maturation step relatively successfully, discrepancies between the neutrophil differentiation system in this study and normal granulopoiesis were noted such as the lower expression of CD16 than that shown by previous reports on hESC-derived neutrophils (Choi et al., 2009; Saeki et al., 2009; Yokoyama et al., 2009). As CD16 is a mature neutrophil marker in peripheral blood, two reasons could explain this phenomenon. First, residual precursors could have been more significant contaminants in the present system than in previously reported methods due to the function of cytokines and stroma supporting immature hematopoietic cells. Another possible reason is the shift of protein types between membrane-bound and soluble forms. Calluri previously reported that G-CSF is not only a myeloid cell growth factor, but also a modulator of neutrophil behavior (Carulli, 1997), and its stimulation decreases the membrane bound CD16 and increases its soluble form. Low CD16 expression has been documented in neutrophils derived in vitro from bone marrow $CD34^+$ cells by stimulation with G-CSF (Kerst et al., 1993b), and it has been observed in vivo when G-CSF is administered to healthy volunteers (Kerst et al., 1993a). This phenomenon, which is also documented in a report of hESC-derived neutrophils (Yokoyama et al., 2009), is unavoidable in differentiation culture systems using recombinant cytokines. The combination of flow cytometric and PCR analyses enables a more accurate staging of progenitors that could be of importance in the investigation of maturation arrest in future studies.

The culture system presented in this study is considered ineligible for clinical applications due to the use of xenogeneic factors such as OP9 cells and FCS. To overcome this problem, a xeno-free hematopoietic differentiation system from pluripotent cells is currently being established.

In conclusion, the present study shows the establishment of a fully functional mature neutrophil differentiation system from hiPSCs and the detailed analysis of their function and differentiation process. This system could become a useful tool for the investigation of various hematological diseases with defects in maturation and function of neutrophils.

Acknowledgments

We thank Dr. Yamanaka for providing the human iPS cell lines 201B6, 253G1, and 253G4, and Dr. Kodama for providing the OP9 cells. We are grateful to Kyowa Hakko Kirin for providing IL-3, TPO, and G-CSF. We also thank the Center for Anatomical Studies, Kyoto University Graduate School of Medicine for immunocytochemical analysis and transmission electron microscopy analysis. This work was supported by grants from the Ministry of Education, Culture, Sports, Science and Technology, Japan. This work was also supported by the Global COE Program "Center for Frontier Medicine" by the Ministry of Education, Culture, Sports, Science, and Technology (MEXT), Japan.

References

Agarwal S, Loh YH, McLoughlin EM, Huang J, Park IH, Miller JD, Huo H, Okuka M, Dos Reis RM, Loewer S, Ng HH, Keefe DL, Goldman FD, Klingelhutz AJ, Liu L, Daley GQ. 2010. Telomere elongation in induced pluripotent stem cells from dyskeratosis congenita patients. Nature 464:292–296.

Alter BP. 2007. Diagnosis, genetics, and management of inherited bone marrow failure syndromes. Hematology Am Soc Hematol Educ Program 29–39.

Borregaard N, Cowland JB. 1997. Granules of the human neutrophilic polymorphonuclear leukocyte. Blood 89:3503–3521.

Borregaard N, Theilgaard-Monch K, Sorensen OE, Cowland JB. 2001. Regulation of human neutrophil granule protein expression. Curr Opin Hematol 8:23–27.

Boyden S. 1962. The chemotactic effect of mixtures of antibody and antigen on polymorphonuclear leucocytes. J Exp Med 115:453–466.

Carulli G. 1997. Effects of recombinant human granulocyte colony-stimulating factor administration on neutrophil phenotype and functions. Haematologica 82:606–616.

Choi KD, Vodyanik MA, Slukvin II. 2009. Generation of mature human myelomonocytic cells through expansion and differentiation of pluripotent stem cell-derived lin-CD34+CD43+CD45+ progenitors. J Clin Invest 119:2818–2829.

Collins SJ, Ruscetti FW, Gallagher RE, Gallo RC. 1978. Terminal differentiation of human promyelocytic leukemia cells induced by dimethyl sulfoxide and other polar compounds. Proc Natl Acad Sci USA 75:2458–2462.

Cowland JB, Borregaard N. 1999. The individual regulation of granule protein mRNA levels during neutrophil maturation explains the heterogeneity of neutrophil granules. J Leukoc Biol 66:989–995.

Duan Z, Horwitz M. 2003. Targets of the transcriptional repressor oncoprotein Gfi-1. Proc Natl Acad Sci USA 100:5932–5937.

Evans MJ, Kaufman MH. 1981. Establishment in culture of pluripotential cells from mouse embryos. Nature 292:154–156.

Friedman AD. 2007. Transcriptional control of granulocyte and monocyte development. Oncogene 26:6816–6828.

Harvath L, Falk W, Leonard EJ. 1980. Rapid quantitation of neutrophil chemotaxis: use of a polyvinylpyrrolidone-free polycarbonate membrane in a multiwell assembly. J Immunol Methods 37:39–45.

Kerst JM, de Haas M, van der Schoot CE, Slaper-Cortenbach IC, Kleijer M, von dem Borne AE, van Oers RH. 1993a. Recombinant granulocyte colony-stimulating factor administration to healthy volunteers: induction of immunophenotypically and functionally altered neutrophils via an effect on myeloid progenitor cells. Blood 82:3265–3272.

Kerst JM, van de Winkel JG, Evans AH, de Haas M, Slaper-Cortenbach IC, de Wit TP, von dem Borne AE, van der Schoot CE, van Oers RH. 1993b. Granulocyte colony-stimulating factor induces hFc gamma RI (CD64 antigen)-positive neutrophils via an effect on myeloid precursor cells. Blood 81:1457–1464.

Kholodnyuk ID, Kozireva S, Kost-Alimova M, Kashuba V, Klein G, Imreh S. 2006. Down regulation of 3p genes, LTF, SLC38A3 and DRR1, upon growth of human chromosome 3-mouse fibrosarcoma hybrids in severe combined immunodeficiency mice. Int J Cancer 119:99–107.

Lensch MW, Daley GQ. 2006. Scientific and clinical opportunities for modeling blood disorders with embryonic stem cells. Blood 107:2605–2612.

Meissner A, Wernig M, Jaenisch R. 2007. Direct reprogramming of genetically unmodified fibroblasts into pluripotent stem cells. Nat Biotechnol 25:1177–1181.

Mori Y, Iwasaki H, Kohno K, Yoshimoto G, Kikushige Y, Okeda A, Uike N, Niiro H, Takenaka K, Nagafuji K, Miyamoto T, Harada M, Takatsu K, Akashi K. 2009. Identification of the human eosinophil lineage-committed progenitor: revision of phenotypic definition of the human common myeloid progenitor. J Exp Med 206:183–193.

Nakagawa M, Koyanagi M, Tanabe K, Takahashi K, Ichisaka T, Aoi T, Okita K, Mochiduki Y, Takizawa N, Yamanaka S. 2008. Generation of induced pluripotent stem cells without Myc from mouse and human fibroblasts. Nat Biotechnol 26:101–106.

Newburger PE, Chovaniec ME, Greenberger JS, Cohen HJ. 1979. Functional changes in human leukemic cell line HL-60. A model for myeloid differentiation. J Cell Biol 82:315–322.

Niwa A, Umeda K, Chang H, Saito M, Okita K, Takahashi K, Nakagawa M, Yamanaka S, Nakahata T, Heike T. 2009. Orderly hematopoietic development of induced pluripotent stem cells via Flk-1(+) hemoangiogenic progenitors. J Cell Physiol 221:367–377.

Okita K, Ichisaka T, Yamanaka S. 2007. Generation of germline-competent induced pluripotent stem cells. Nature 448:313–317.

Park IH, Arora N, Huo H, Maherali N, Ahfeldt T, Shimamura A, Lensch MW, Cowan C, Hochedlinger K, Daley GQ. 2008a. Disease-specific induced pluripotent stem cells. Cell 134:877–886.

Park IH, Zhao R, West JA, Yabuuchi A, Huo H, Ince TA, Lerou PH, Lensch MW, Daley GQ. 2008b. Reprogramming of human somatic cells to pluripotency with defined factors. Nature 451:141–146.

Raya A, Rodriguez-Piza I, Guenechea G, Vassena R, Navarro S, Barrero MJ, Consiglio A, Castella M, Rio P, Sleep E, Gonzalez F, Tiscornia G, Garreta E, Aasen T, Veiga A, Verma IM, Surralles J, Bueren J, Izpisua Belmonte JC., 2009. Disease-corrected haematopoietic progenitors from Fanconi anaemia induced pluripotent stem cells. Nature 460:53–59.

Saeki K, Nakahara M, Matsuyama S, Nakamura N, Yogiashi Y, Yoneda A, Koyanagi M, Kondo Y, Yuo A. 2009. A feeder-free and efficient production of functional neutrophils from human embryonic stem cells. Stem Cells 27:59–67.

Shinoda G, Umeda K, Heike T, Arai M, Niwa A, Ma F, Suemori H, Luo HY, Chui DH, Torii R, Shibuya M, Nakatsuji N, Nakahata T. 2007. alpha4-Integrin(+) endothelium derived from primate embryonic stem cells generates primitive and definitive hematopoietic cells. Blood 109:2406–2415.

Sugimoto C, Fujieda S, Sunaga H, Noda I, Tanaka N, Kimura Y, Saito H, Matsukawa S. 2001. Granulocyte colony-stimulating factor (G-CSF)-mediated signaling regulates type IV collagenase activity in head and neck cancer cells. Int J Cancer 93:42–46.